Cell Reports

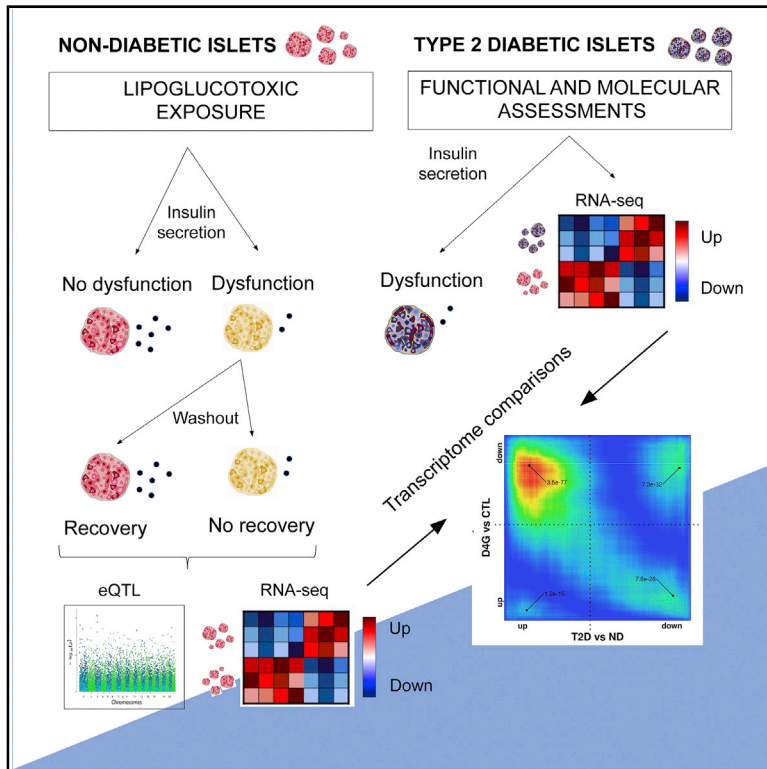# Persistent or Transient Human β Cell Dysfunction Induced by Metabolic Stress: Specific Signatures and Shared Gene Expression with Type 2 Diabetes

Graphical Abstract

Authors

Lorella Marselli, Anthony Piron, Mara Suleiman, ..., Decio L. Eizirik, Miriam Cnop, Piero Marchetti

Correspondence

lorella.marselli@med.unipi.it (L.M.), mcnop@ulb.ac.be (M.C.), piero.marchetti@med.unipi.it (P.M.)

In Brief

Marselli et al. find that human β cell dysfunction induced by metabolic stresses is persistent or transient. RNA sequencing and eQTL analysis identify key pathways underlying failure and recovery. Type 2 diabetes β cells have several functional and molecular alterations and share specific transcriptomic traits of β cells with irreversible or rescuable damage.

Highlights

- Human β cell dysfunction induced by metabolic stress may be persistent or transient

- Specific transcriptomic changes associate with durable or reversible damage

- Type 2 diabetes (T2D) β cells have several functional and molecular alterations

- T2D and irreversibly or temporarily impaired β cells share key transcriptome traits

Article

Persistent or Transient Human β Cell Dysfunction Induced by Metabolic Stress: Specific Signatures and Shared Gene Expression with Type 2 Diabetes

Lorella Marselli,[1,*] Anthony Piron,[2] Mara Suleiman,[1] Maikel L. Colli,[2] Xiaoyan Yi,[2] Amna Khamis,[3] Gaelle R. Carrat,[4] Guy A. Rutter,[4,5] Marco Bugliani,[1] Laura Giusti,[1,6] Maurizio Ronci,[7,8] Mark Ibberson,[9] Jean-Valery Turatsinze,[2] Ugo Boggi,[10,11] Paolo De Simone,[10,12] Vincenzo De Tata,[10] Miguel Lopes,[2] Daniela Nasteska,[2] Carmela De Luca,[1] Marta Tesi,[1] Emanuele Bosi,[1] Pratibha Singh,[2] Daniela Campani,[13] Anke M. Schulte,[14] Michele Solimena,[15,16] Peter Hecht,[14] Brian Rady,[17] Ivona Bakaj,[17] Alessandro Pocai,[17] Lisa Norquay,[17] Bernard Thorens,[18] Mickaël Canouil,[3] Philippe Froguel,[19] Decio L. Eizirik,[2,20,21,22] Miriam Cnop,[2,22,23,*] and Piero Marchetti[1,23,24,*]

[1]Department of Clinical and Experimental Medicine, and AOUP Cisanello University Hospital, University of Pisa, Pisa 56126, Italy
[2]ULB Center for Diabetes Research, Université Libre de Bruxelles, Brussels 1070, Belgium
[3]INSERM UMR 1283, CNRS UMR 8199, European Genomic Institute for Diabetes (EGID), Institut Pasteur de Lille, University of Lille, Lille University Hospital, Lille 59000, France
[4]Section of Cell Biology and Functional Genomics, Division of Diabetes, Endocrinology, and Metabolism, Imperial College, London, UK
[5]Lee Kong Chian School of Medicine, Nanyang Technological University, Singapore, Singapore
[6]School of Pharmacy, University of Camerino, Camerino, Italy
[7]Department of Pharmacy, University "G. d'Annunzio" of Chieti-Pescara, Chieti, Italy
[8]Centre for Advanced Studies and Technologies (CAST), University "G. d'Annunzio" of Chieti-Pescara, Chieti, Italy
[9]Vital-IT Group, Swiss Institute of Bioinformatics, Lausanne 1015, Switzerland
[10]Department of Translational Research and New Technologies in Medicine and Surgery, University of Pisa, Pisa 56126, Italy
[11]Division of General and Transplant Surgery, Cisanello University Hospital, Pisa 56124, Italy
[12]Division of Liver Surgery and Transplantation, Cisanello University Hospital, Pisa 56124, Italy
[13]Department of Surgical, Medical and Molecular Pathology and the Critical Areas, University of Pisa, Pisa 56126, Italy
[14]Sanofi-Aventis Deutschland GmbH, Diabetes Research, Frankfurt, Germany
[15]Paul Langerhans Institute Dresden of the Helmholtz Center Munich at University Hospital Carl Gustav Carus and Faculty of Medicine, TU Dresden, Dresden 01307, Germany
[16]German Center for Diabetes Research (DZD e.V.), Neuherberg 85764, Germany
[17]Janssen RDUS, Philadelphia, PA, USA
[18]Center for Integrative Genomics, University of Lausanne, Lausanne, Switzerland
[19]Department of Metabolism, Digestion, and Reproduction, Imperial College London, London, UK
[20]WELBIO, Université Libre de Bruxelles, Brussels, Belgium
[21]Indiana Biosciences Research Institute, Indianapolis, IN, USA
[22]Division of Endocrinology, ULB Erasmus Hospital, Université Libre de Bruxelles, Brussels, Belgium
[23]These authors contributed equally
[24]Lead Contact
*Correspondence: lorella.marselli@med.unipi.it (L.M.), mcnop@ulb.ac.be (M.C.), piero.marchetti@med.unipi.it (P.M.)
https://doi.org/10.1016/j.celrep.2020.108466

SUMMARY

Pancreatic β cell failure is key to type 2 diabetes (T2D) onset and progression. Here, we assess whether human β cell dysfunction induced by metabolic stress is reversible, evaluate the molecular pathways underlying persistent or transient damage, and explore the relationships with T2D islet traits. Twenty-six islet preparations are exposed to several lipotoxic/glucotoxic conditions, some of which impair insulin release, depending on stressor type, concentration, and combination. The reversal of dysfunction occurs after washout for some, although not all, of the lipoglucotoxic insults. Islet transcriptomes assessed by RNA sequencing and expression quantitative trait loci (eQTL) analysis identify specific pathways underlying β cell failure and recovery. Comparison of a large number of human T2D islet transcriptomes with those of persistent or reversible β cell lipoglucotoxicity show shared gene expression signatures. The identification of mechanisms associated with human β cell dysfunction and recovery and their overlap with T2D islet traits provide insights into T2D pathogenesis, fostering the development of improved β cell-targeted therapeutic strategies.

INTRODUCTION

Pancreatic β cell failure, due to the interplay of genetic and acquired factors, is key to the onset and progression of type 2 diabetes (T2D) (Kahn, 2003; Cnop et al., 2005; Marchetti et al., 2009; Ferrannini, 2010; Ashcroft and Rorsman, 2012; Halban et al., 2014; Accili et al., 2016; Fuchsberger et al., 2016; Yang et al., 2018; Miguel-Escalada et al., 2019). Since the UK Prospective Diabetes Study (UK Prospective Diabetes Study [UKPDS] Group, 1998), it has been assumed that the decline of β cell functional mass begins before the onset of T2D and proceeds relentlessly thereafter, leading to worsening of glycemic control and requiring progressive intensification of diabetes therapy. The causes of this deterioration are not completely understood, but prolonged exposure to saturated fatty acids (lipotoxicity), high glucose (glucotoxicity) or combinations thereof (lipoglucotoxicity) may contribute to β cell failure via several different mechanisms (Lupi et al., 2002; Robertson et al., 2004; Cunha et al., 2008; Weir et al., 2009; Robertson, 2009; Wiederkehr and Wollheim, 2009; Poitout et al., 2010; Bensellam et al., 2012; Cnop et al., 2014; Ottosson-Laakso et al., 2017; Coomans de Brachene et al., 2018; Hall et al., 2019; Eizirik et al., 2020; Marchetti et al., 2020).

Growing evidence shows that the alleviation of metabolic stress can improve β cell function. Pharmacological reduction of free fatty acid levels in non-diabetic (ND) first-degree relatives of T2D individuals led to better insulin release during hyperglycemic clamp (Cusi et al., 2007). Acute insulin response to intravenous glucose in healthy subjects was reduced after long-term fatty acid infusion, and recovered 24 h after discontinuation of lipid administration (Paolisso et al., 1995). Low-calorie diet, glucose-lowering drugs, or bariatric surgery have resulted in diabetes remission and/or improved insulin secretion in sizeable proportions of T2D subjects (Kosaka et al., 1980; Camastra et al., 2013; Mingrone et al., 2015; White et al., 2016; Steven et al., 2016; Taylor et al., 2018; Lean et al., 2018).

The trajectory and molecular mechanisms of human β cell dysfunction, which may include possible reversal of damage, following different metabolic stresses remain to be fully clarified, however. Previous work has shown that isolated human islets exposed for a few days to high glucose concentrations lost β cell sensitivity to subsequent acute glucose stimulation, which was partially restored after additional culture in medium at near-physiological glucose concentrations (~5.5 mmol/L) (Davalli et al., 1991; Eizirik et al., 1992; Marshak et al., 1999). The mechanisms underlying the persistence or transience of human β cell defects during lipoglucotoxicity are unknown and, crucially, it has not been determined to what extent the alterations induced by metabolic stress and their possible recovery in ND islets reflect those of islets from T2D individuals.

We performed a comprehensive study (Figure 1) with a large number (n = 26) of human islet preparations (Table S1) to assess the direct impact of different lipoglucotoxic treatments on β cell function and evaluated whether the deleterious effects were persistent or reversible after washout. The *ex vivo* lipoglucotoxic treatments were selected to reflect biologically relevant concentrations of the most common saturated and mono-unsaturated fatty acid and glucose (methodological considerations are reviewed in Lytrivi et al., 2020). For key conditions, islet transcrip-

tome and genome were analyzed by RNA sequencing (RNA-seq) and expression quantitative trait loci (eQTL) to unveil the possibly involved molecular mechanisms. Finally, the molecular changes associated with persistent or transient β cell dysfunction were correlated with those of islets from 28 T2D donors compared with 58 ND subjects (Table S1). The present identification of mechanisms responsible for human β cell functional deterioration and rescue and their overlap with T2D islet traits provide insights into T2D pathogenesis and should foster the development of improved β cell targeted therapeutic strategies.

RESULTS

Differential Impact of Lipoglucotoxic Conditions on β Cell Function

We evaluated glucose-stimulated insulin secretion (GSIS) of human islets under control or lipoglucotoxic conditions (Figure 1) and found that the impact of metabolic stress and washout varied across experimental settings. In islets cultured at 11.1 mmol/L glucose (g), 1.0 mmol/L palmitate+oleate (P+O; 1:2 molar ratio), or 1.0 mmol/L palmitate+oleate+11.1 mmol/L glucose (P+O+g), glucose-induced insulin release did not differ as compared to islets cultured in control medium (5.5 mmol/L glucose), and was similar at day 2 (D2; basal), D4 (stress), and D8 (after washout) (Figure S1A). However, the islets cultured at 0.5 mmol/L palmitate (P), 22.2 mmol/L glucose (G), 0.5 mmol/L palmitate+11.1 mmol/L glucose (P+g), 0.5 mmol/L palmitate+22.2 mmol/L glucose (P+G), or 1.0 mmol/L palmitate+oleate+22.2 mmol/L glucose (P+O+G) showed, at D4, several changes in GSIS (Figure 2). Specifically, 0.5 mmol/L palmitate (P and P+g) induced a trend to lower insulin release in response to acute stimulation with high (16.7 mmol/L) glucose (Figures 2A and 2C). Two-day incubation with G was associated with a tendency to a higher insulin secretion at low (3.3 mmol/L) glucose and blunted release in response to 16.7 mmol/L glucose (Figure 2B). Previous exposure to combined palmitate and high glucose (P+G and P+O+G) induced increased insulin secretion at low glucose but a less affected response to increased glucose level (Figures 2D and 2E). These alterations led to significant reduction of the insulin stimulation index (ISI) at D4 in all 5 conditions, in comparison with the respective controls (Figures 2F–2J).

GSIS improved after washout of P, G, and P+g, so that no significant differences persisted at D8 in comparison with control islets (Figures 2A–C and 2F–2H). On the contrary, with the lipoglucotoxic conditions P+G or P+O+G, the secretory dysfunction persisted despite the washout (D8) (Figures 2D, 2E, 2I, and 2J).

Over the 8-day incubation time, islet insulin content decreased significantly (Figure S1B). In control islets, it tended to be lower at D4 (~−15%) and was significantly reduced at D8 versus D2 (~−30%, p < 0.01) (Figure S1B). Insulin content was not available for the islets exposed to g. For those incubated with P+O and P+O+g (not associated with any change of insulin release), the reduction in insulin content resembled that of control islets (Figure S1B). For the culture conditions causing dysfunction (P, G, P+g, P+G, and P+O+G), a markedly lower insulin content (<50%) was already seen at D4, which remained reduced at D8 (Figure S1B). When ISI values were normalized at each time point to the respective islet insulin content, the results
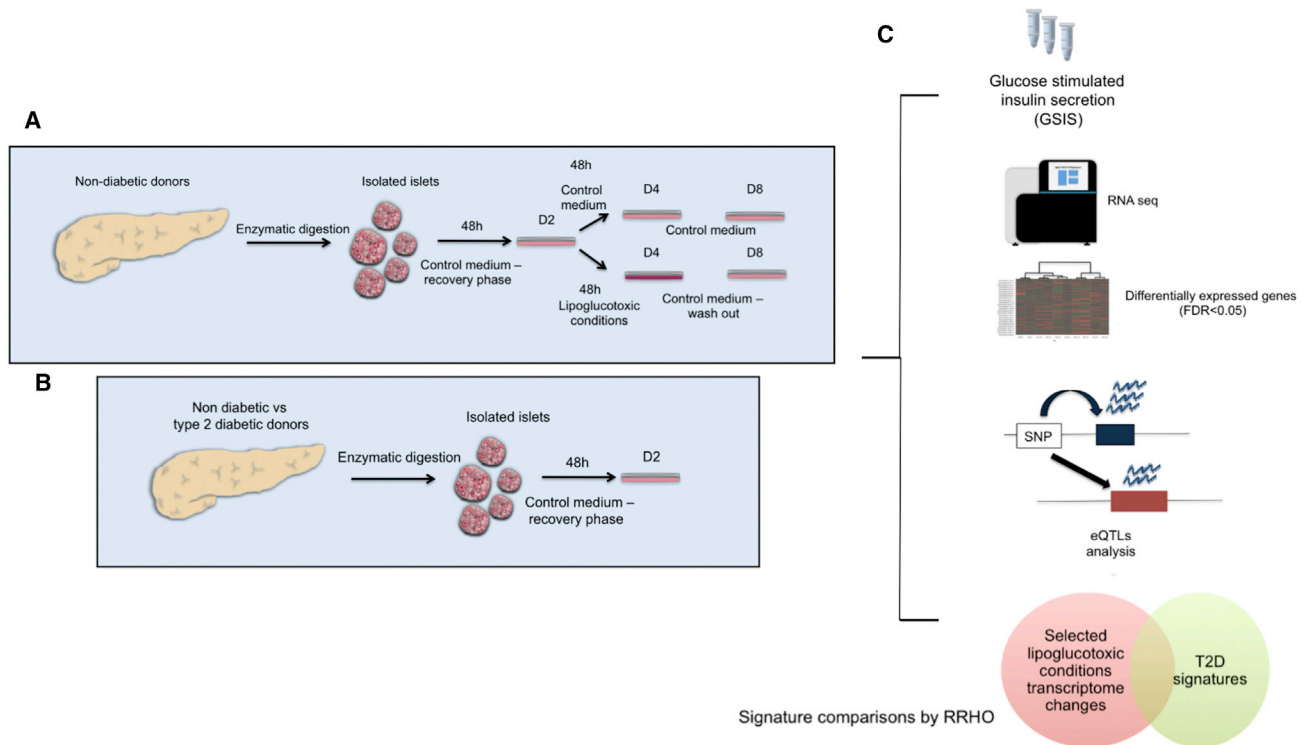
Figure 1. Schematic Representation of the Research Approach
(A) Islets were isolated from the pancreas of non-diabetic (ND) donors, and after 2 days in culture in control medium (glucose concentration 5.5 mmol/L, to allow recovery from the digestion/purification stress) (day [D] 2), they were cultured for 2 additional days (D4) in control medium or in the presence of lipotoxic and/or glucotoxic conditions. Then, the stressful conditions were removed and islets were cultured in control medium for 4 days (washout, D8).
(B) Islets were prepared from the pancreas of ND (independent samples) and type 2 diabetic (T2D) donors, and were allowed to recover after the isolation (D2).
(C) Studies were performed with ND islets (control or lipotoxicity-exposed, including washout) at D2, D4, and D8, and with ND and T2D islets at D2. RRHO, rank-rank hypergeometric overlap.

(Figure S1C) confirmed those obtained with the actual insulin secretion values (see Figures 2 and S1).

Light and electron microscopy assessments were performed in selected experiments. In the P alone series, the islets had preserved architecture at the different time points (D2, D4, and D8), as shown by chomogranin A and insulin and glucagon staining (Figure S2A). β cell apoptosis was evaluated in P-exposed islets (decreased insulin release at D4 and recovery after washout; 427 β cells from 6 islets of 2 different preparations) and P+O+G-exposed islets (decreased insulin release at D4 and persistence of impairment after washout; 582 β cells from 6 islets of 2 separate preparations). With P (Figure S2B), the proportion of apoptotic β cells increased from $0.61\% \pm 0.1\%$ at D2 to $4.28\% \pm 0.35\%$ at D4 ($p < 0.05$ after Bonferroni correction), and then decreased after washout ($1.08\% \pm 0.27\%$). With P+O+G, no significant change occurred in β cell apoptosis ($0.55\% \pm 0.14\%$ at D2; $1.85\% \pm 0.44\%$ at D4; and $1.07\% \pm 0.29\%$ at D8 washout). Although these results were obtained with a fraction of all of the samples studied and may not be representative of all of the islets assayed in the secretion studies, they suggest that the changes in GSIS after P or P+O+G exposure were unlikely due to a major loss of β cells. However, more work is needed to evaluate β cell death/survival over the time under lipoglucotoxic conditions and assess the effect of wash-out incubations.

In summary, acute GSIS from human islets was impaired after prolonged exposure to some of the tested lipotoxic and/or glucotoxic conditions. The removal of metabolic stress led to recovery from the damage induced by P or G alone, while β cell dysfunction persisted when the fatty acid and high glucose were combined.

RNA-Seq of P-Treated Human Islets
We then explored whether and how the functional changes were associated with modifications in islet transcriptomes (Figure 1). We focused on P-exposed islets, which had altered GSIS (D4) and recovered after washout (D8). Compared to control islets at D4, P-treated islets had 646 differentially (false discovery rate [FDR] < 0.05) expressed genes (272 upregulated and 374 downregulated; Table S2A). Of these, 595 were protein-coding genes (248 upregulated and 347 downregulated by P). The top 20 upregulated and downregulated protein-coding genes (Table 1) included genes involved in lipid metabolism (e.g., *ACSL1*, the fatty acid desaturases *SCD*, *FADS1*, *FADS2*), inflammation (comprising *IGSF6*, *AIF1*, and *TRIB3*), and other cell functions. Overall, the results are in keeping with previous RNA-seq or microarray transcriptome analyses of P-exposed human islets (Cnop et al., 2014; Hall et al., 2014). We next performed enrichment analysis for high-throughput data interpretation using
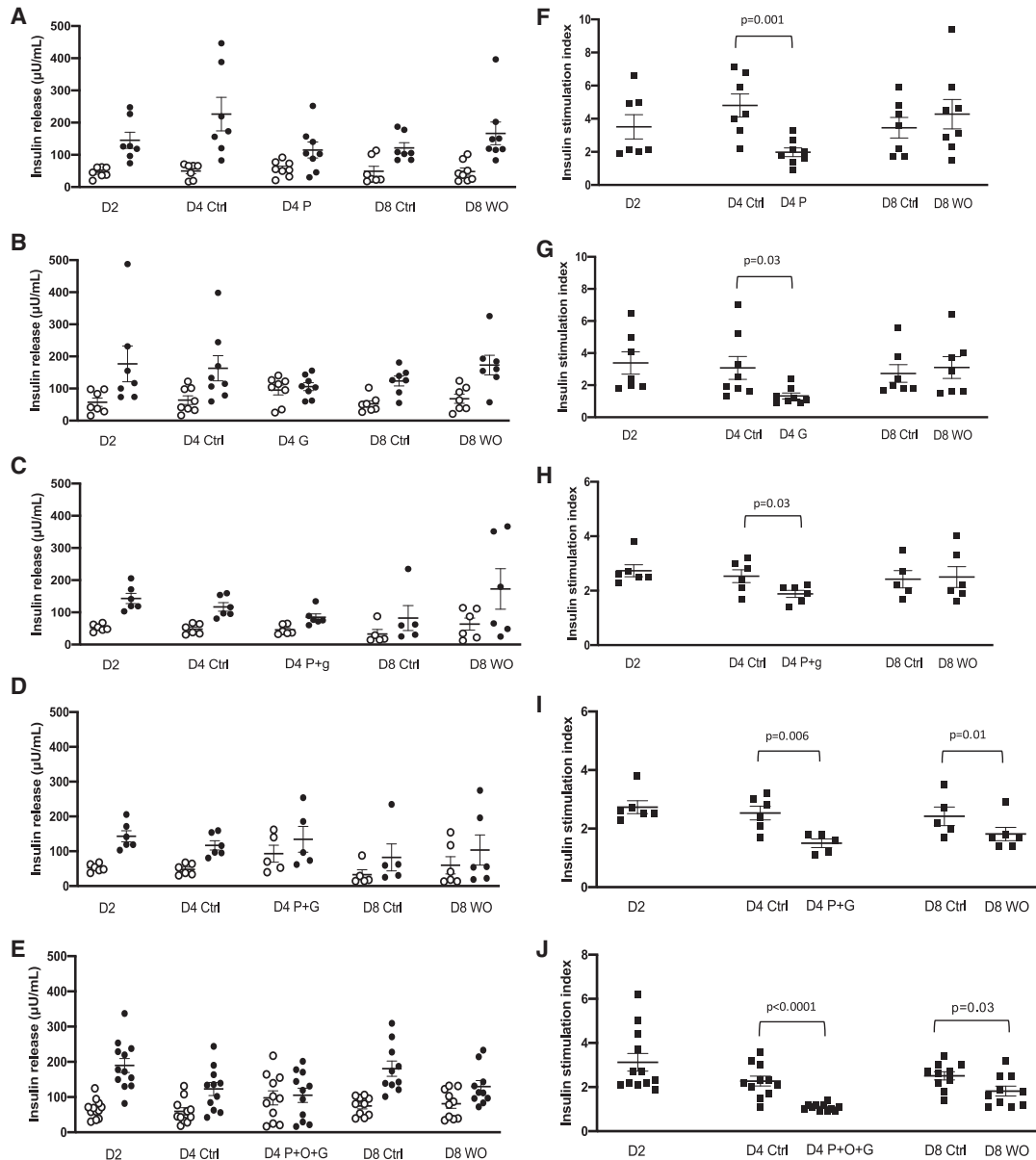
Figure 2. Glucose-Stimulated (3.3 and 16.7 mmol/L Glucose) Insulin Secretion from Human Islets Basally (D2), after 2 Days of Incubation at the Indicated Metabolically Stressful Conditions (D4) and after 4 Days of Washout (D8 WO)

Ctrl indicates islets cultured at normal (5.5 mmol/L) glucose level throughout the study.

(A–E and G) At D4: incubation with 0.5 mmol/L palmitate (P) and P+11.1 mmol/L glucose (P+g) induced a trend to lower insulin release in response to acute stimulation with high (16.7 mmol/L) glucose (A and C); incubation with 22.2 mmol/L glucose (G) was associated with a tendency to higher insulin secretion in response to low (3.3 mmol/L) glucose and blunted release in response to 16.7 mmol/L glucose (B); incubation with combined 0.5 mmol/L P or 1.0 mmol/L P+O (1:2 ratio) and 22.2 mmol/L glucose (P+G and P+O+G) was associated with increased insulin secretion at low glucose but a less affected response to high glucose (D and E).

(F–J) Consequently, at D4 the insulin stimulation index was lower at all these five conditions, compared to the respective controls. At D8: GSIS improved after washout of P, G, and P+g (A–C and F–H), whereas with P+G and 1.0 mmol/L P+O+ 22.2 mmol/L glucose, the secretory dysfunction persisted despite the washout (D8) (D, E, I, and J). The number of separate islet preparations and the number of replicates per condition were for P, 4 and 7/8 per time point (37 replicates in total); for G, 4 and 7/8 per time point (37 replicates in total); for P+g, 3 and 5/6 per time point (29 replicates in total); for P+G, 3 and 5/6 per time point (28 replicates in total); for P+O+G, 6 and 10/12 per time point (54 replicates in total).

Bars indicate means ± SEs.

Table 1. Top 20 Upregulated and Dowregulated Genes in 0.5 mM Palmitate Washout Islets (D8) versus 0.5 mM Palmitate-Exposed Islets (D4)

Gene ID	Gene Symbol	Gene Name	Median D4P	Median D8P	log$_2$FC	FDR_BH
Upregulated Genes						
ENSG00000179934	CCR8	C-C motif chemokine receptor 8	0.00	1.72	11.56	3.61E−33
ENSG00000168453	HR	HR lysine demethylase and nuclear receptor corepressor	0.15	1.52	3.02	2.31E−11
ENSG00000116032	GRIN3B	glutamate ionotropic receptor NMDA type subunit 3B	0.05	0.44	2.67	1.12E−10
ENSG00000120693	SMAD9	SMAD family member 9	1.66	5.31	1.56	7.73E−10
ENSG00000121207	LRAT	lecithin retinol acyltransferase	0.23	0.85	1.97	1.19E−9
ENSG00000104953	TLE6	TLE family member 6, subcortical maternal complex member	2.24	7.19	2.12	1.34E−8
ENSG00000117472	TSPAN1	tetraspanin 1	20.13	92.06	1.71	2.43E−7
ENSG00000168234	TTC39C	tetratricopeptide repeat domain 39C	5.87	12.55	1.29	3.71E−7
ENSG00000166833	NAV2	neuron navigator 2	7.26	17.39	1.19	8.43E−7
ENSG00000124253	PCK1	phosphoenolpyruvate carboxykinase 1	0.98	6.37	1.93	9.06E−7
ENSG00000137101	CD72	CD72 molecule	5.03	16.03	1.42	2.36E−6
ENSG00000120913	PDLIM2	PDZ and LIM domain 2	8.62	19.37	1.36	4.86E−6
ENSG00000118495	PLAGL1	PLAG1 like zinc finger 1	8.4	16	1.01	1.11E−5
ENSG00000180875	GREM2	gremlin 2, DAN family BMP antagonist	0.7	2.58	1.93	2.14E−5
ENSG00000125968	ID1	inhibitor of DNA binding 1, HLH protein	3.62	24.16	2.26	2.94E−5
ENSG00000162076	FLYWCH2	FLYWCH family member 2	6.86	13.48	1.07	4.86E−5
ENSG00000117318	ID3	inhibitor of DNA binding 3, HLH protein	7.91	34.93	1.99	5.75E−5
ENSG00000183734	ASCL2	achaete-scute family bHLH transcription factor 2	0.49	1.71	1.64	1.26E−4
ENSG00000168874	ATOH8	atonal bHLH transcription factor 8	0.31	1.22	2.65	2.22E−4
ENSG00000141655	TNFRSF11A	TNF receptor superfamily member 11a	3.03	5.66	0.91	2.33E−4
Downregulated Genes						
ENSG00000114771	AADAC	arylacetamide deacetylase	12.19	1.4	−3.29	5.86E−30
ENSG00000135842	FAM129A	niban apoptosis regulator 1	10.88	1.63	−2.71	8.13E−19
ENSG00000142677	IL22RA1	interleukin 22 receptor subunit alpha 1	5.48	0.34	−3.34	7.07E−14
ENSG00000128567	PODXL	podocalyxin-like	5.94	1.46	−1.63	6.99E−12
ENSG00000171766	GATM	glycine amidinotransferase	108.24	29.18	−2.18	1.56E−11
ENSG00000168077	SCARA3	scavenger receptor class A member 3	2.17	0.26	−3.37	1.78E−11
ENSG00000133816	MICAL2	Microtubule-associated monooxygenase, calponin and LIM domain containing 2	12.71	3.71	−1.7	2.31E−11
ENSG00000215704	CELA2B	Chymotrypsin-like elastase 2B	46.44	1.36	−4.59	2.76E−11
ENSG00000109084	TMEM97	transmembrane protein 97	18.15	5.46	−1.49	2.94E−11
ENSG00000120057	SFRP5	secreted frizzled related protein 5	8.73	1.95	−2.23	4.46E−11
ENSG00000164266	SPINK1	serine peptidase inhibitor, Kazal type 1	2,754.32	754.88	−1.54	9.84E−11
ENSG00000060566	CREB3L3	cAMP-responsive element binding protein 3-like 3	0.47	0.08	−2.72	3.21E−10
ENSG00000186480	INSIG1	Insulin-induced gene 1	120.33	40.2	−1.52	4.42E−10
ENSG00000152377	SPOCK1	SPARC (osteonectin), cwcv and kazal-like domains proteoglycan 1	4.32	1.6	−1.87	1.29E−9
ENSG00000109072	VTN	vitronectin	9.54	3.75	−1.69	2.17E−9
ENSG00000123500	COL10A1	collagen type X alpha 1 chain	3.02	0.32	−3.57	2.45E−9
ENSG00000170890	PLA2G1B	phospholipase A2 group IB	1,018.46	67.97	−3.4	1.49E−8
ENSG00000136160	EDNRB	endothelin receptor type B	0.95	0.26	−2.04	1.84E−8
ENSG00000172023	REG1B	regenerating family member 1 beta	5,892.03	252.59	−3.03	2.62E−8
ENSG00000115386	REG1A	regenerating family member 1 alpha	15,289.61	1,373.15	−2.34	3.03E−8

cAMP, cyclic AMP; TNF, tumor necrosis factor.
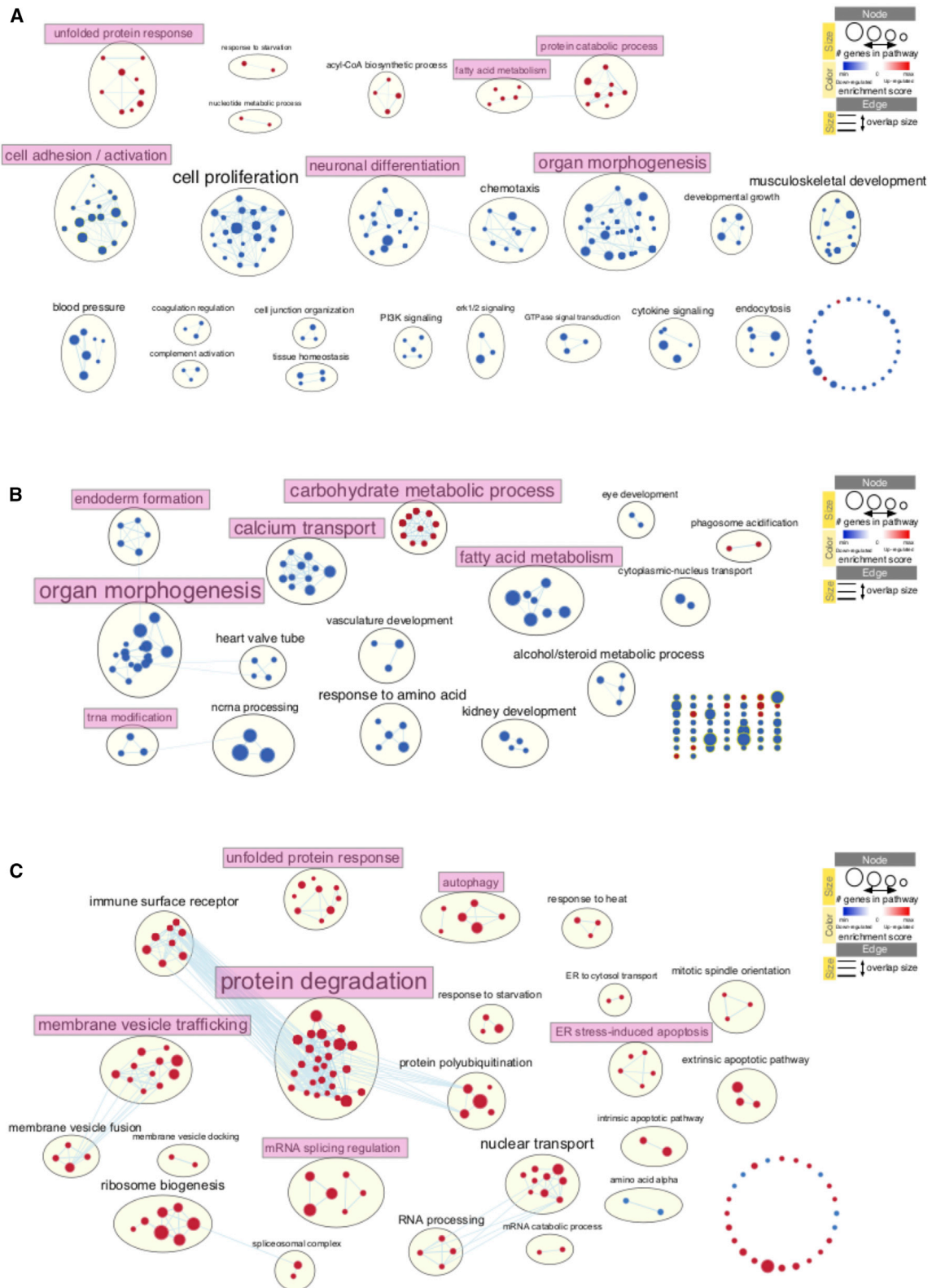
(legend on next page)

Enrichment Map software (Merico et al., 2010). This approach organizes gene sets into networks, connecting them in the map if they have high overlap. We identified several P-modified functional categories (Figure 3A), including the upregulation of unfolded protein response, acyl-coenzyme A (CoA) biosynthesis, and fatty acid metabolism, as well as protein catabolic process, and the downregulation of cell adhesion/activation, neuronal differentiation, and organ morphogenesis. The gene sets and individual genes in these categories are shown in Data S1A.

To assess the transcriptome changes underlying the functional recovery after P washout, we compared the RNA-seq data of D8 washout versus D4 P-treated islets. The genes differentially (FDR < 0.05) expressed were 714 (167 upregulated and 547 downregulated; Table S2B). Of these, 656 were protein coding (142 upregulated and 514 downregulated). Table 1 shows the 20 most differentially upregulated and downregulated genes, having roles in lipid/glucose metabolism (e.g., *PCK1*, *CYP26B1*, *INSIG1*), transcription (including *SMAD9*, *ID1*, *ID3*, and *CREB3L3*), inflammation (*CCR8* and *IL22RA1*), cell growth/development (*TSPAN1*, *GREM2*, *REG1A*, and *REG1B*), β cell function (*SFRP5*), redox balance (*SCARA3*), and others. The Enrichment Map showed changes in several processes in D8 washed-out islets, in particular, downregulation of fatty acid metabolism and upregulation of carbohydrate catabolic processes (Figure 3B; Data S1B).

These RNA-seq transcriptome findings extend previous observations showing that β cell damage due to prolonged P exposure associates with alterations of key cellular processes, and indicate that recovered β cell glucose responsiveness was accompanied by the modification of several pathways, including adaptation from fatty acid to carbohydrate utilization metabolism.

RNA-Seq of High-Glucose-Treated Human Islets

Exposure of human islets to G impaired GSIS at D4, with recovery after washout (D8). Compared with control islets at D4, G-exposed islets had 50 differentially (FDR < 0.05) expressed genes (38 upregulated and 12 downregulated; Table S2C). Among these genes, 42 were protein coding (32 upregulated and 10 downregulated by high glucose). The top upregulated and downregulated protein-coding genes included genes involved in metabolic pathways (*AMY2B*, *ASNS*, and *PIPOX*), gated channel activity (*CHRNA5* and *GLRA1*), and other cell functions. Enrichment Map analysis showed the inhibition of cell junction and metabolic processes (Figure S3A).

To reveal the transcriptome changes after washout of high glucose, we compared the RNA-seq data of D8 washout versus D4 G-treated islets, resulting in 341 differentially expressed genes (FDR < 0.05) (81 upregulated and 260 downregulated; Table S2D). Of these, 320 were protein coding (70 upregulated and 250 downregulated). The 20 most upregulated and downregulated genes play roles in extracellular organization (*MMP9*,

COL7A1, and *POSTN*), establishment of protein localization to the endoplasmic reticulum (ER) (*CHMP4A*), and glycerophospholipid metabolism (*JMJD7*). The Enrichment Map showed downregulation of response to wounding, myeloid cell differentiation, and chemotaxis (Figure S3A).

RNA-Seq of P+G-Treated Human Islets

More profound changes in islet transcriptome were observed with combined P+G. Two-day exposure to this condition (D4) resulted in the differential expression of 1,498 genes (756 upregulated and 742 downregulated; Table S2E). Of these, 1,386 were protein coding (699 upregulated and 687 downregulated). The top 20 upregulated and downregulated genes (Table 2) were related to transcription (e.g., *ATF3*, *MAFF*), inflammation (*CXCL2*, *CXCL8*, and *TRIB3*), cell turnover (*INHBE*), ion channels/transporters (*KCNE4*, *SLC5A4*), mitochondrial function (*GATM*), and redox balance (comprising *GSTA1* and *GSTA2*). The Enrichment Map showed the clustering of interrelated gene sets, the majority of which were upregulated (Figure 3C). The most relevant ones comprised unfolded protein response, protein degradation, mRNA splicing regulation, and ER stress-induced apoptosis (Data S1C). In line with the persistence of β cell dysfunction after P+G washout (Figure 2D), the RNA-seq data of human islets at D8 washout versus D4 identified only 322 genes differentially expressed (120 upregulated and 202 downregulated). Of these, 292 were protein coding (102 upregulated and 190 downregulated; Table S2F). These results indicate that under this lipoglucotoxic condition, key β cell pathways are deeply altered and fail to recover after the removal of metabolic stress, contributing to the persistence of β cell dysfunction.

Comparison of P, G, and P+G Exposure

We next compared similarities and differences between these models of nutrient oversupply (single or combined). When comparing G with the P and P+G lipotoxic conditions, only a few differentially expressed genes overlapped, while 209 genes overlapped between the 2 lipotoxic conditions (Figure S4A). The full list of these genes is provided in Table S2G. Interestingly, the extent of transcriptome alterations reflected the changes of the β cell functional phenotype (P+G > P > G). We further compared the functional enrichment terms among these 3 stress conditions (Figures S4B and S4C). P and P+G shared 19 upregulated terms, G and P+G shared only 1, and no term was shared between G or P (Table S2H). P and P+G strongly overlapped in the ER stress response, with half of the shared terms pertaining to this pathway (Table S2H). For the downregulated terms, G and P shared 5 downregulated terms (related to cell junction). P and P+G and G and P+G each shared only 1 term (Table S2I).

Evidence for β Cell Differentiation with Lipotoxicity

Dedifferentiation is a biological phenomenon associated with the loss of specialized function. By comparing β cell disallowed (or

---

Figure 3. Enrichment Map Analysis of the Transcriptome
(A) Islets exposed to 0.5 mmol/L P versus control islets at D4.
(B) Islets previously exposed to 0.5 mmol/L P and then washed out (D8) versus P-exposed islets (D4).
(C) Islets exposed to 0.5 mmol/L P + 22.2 mmol/L glucose versus control islets at D4.
Red indicates upregulated and blue indicates downregulated processes.

Table 2. Top 20 Upregulated and Downregulated Genes in 0.5 mM Palmitate Plus High-Glucose-Treated Islets (D4) versus Not Exposed Islets (D4)

Gene ID	Gene Symbol	Gene Name	Median D4C	Median D4PG	log$_2$FC	FDR_BH
Upregulated Genes						
ENSG00000169429	CXCL8	C-X-C motif chemokine ligand 8	55.41	277.8	2.57	1.05E−49
ENSG00000143333	RGS16	regulator of G protein signaling 16	6.56	29.86	2.29	5.55E−38
ENSG00000162772	ATF3	activating transcription factor 3	14.06	70.06	2.24	4.61E−36
ENSG00000152049	KCNE4	potassium voltage-gated channel subfamily E regulatory subunit 4	4.13	20.09	2.17	4.77E−29
ENSG00000139269	INHBE	inhibin subunit beta E	1.18	5.98	3	2.35E−22
ENSG00000087074	PPP1R15A	protein phosphatase 1 regulatory subunit 15A	28.77	124.87	1.76	6.43E−22
ENSG00000197279	ZNF165	zinc finger protein 165	3.48	14.61	1.87	1.89E−20
ENSG00000162873	KLHDC8A	kelch domain containing 8A	11.08	31.99	1.56	4.48E−20
ENSG00000167772	ANGPTL4	angiopoietin-like 4	0.65	7.62	3.62	1.54E−19
ENSG00000101255	TRIB3	tribbles pseudokinase 3	19.71	62.84	1.47	2.41E−19
ENSG00000172432	GTPBP2	GTP binding protein 2	28.02	73.95	1.23	3.24E−19
ENSG00000108176	DNAJC12	DnaJ heat shock protein family (Hsp40) member C12	66.05	151.14	1.2	2.38E−17
ENSG00000100191	SLC5A4	solute carrier family 5 member 4	1.13	4.52	2.19	2.86E−17
ENSG00000137331	IER3	immediate early response 3	47.41	266.02	2.02	5.63E−17
ENSG00000185022	MAFF	MAF bZIP transcription factor F	7.29	22.07	1.49	1.99E−15
ENSG00000081041	CXCL2	C-X-C motif chemokine ligand 2	12.48	35.98	1.38	2.38E−15
ENSG00000147872	PLIN2	perilipin 2	8.1	30.51	2.31	4.92E−15
ENSG00000175592	FOSL1	FOS-like 1, AP-1 transcription factor subunit	1.75	7.65	2.15	7.37E−15
ENSG00000177426	TGIF1	TGF-β-induced factor homeobox 1	23.78	48.49	1.25	7.95E−15
ENSG00000130766	SESN2	sestrin 2	15.73	36.58	1.26	2.76E−14
Downregulated Genes						
ENSG00000248144	ADH1C	alcohol dehydrogenase 1C (class I), gamma polypeptide	81.73	26.49	−1.53	2.10E−26
ENSG00000259171	AL163636.2	uncharacterized protein	3.64	0.38	−3.03	1.11E−21
ENSG00000171766	GATM	glycine amidinotransferase	106.63	25.69	−1.79	1.19E−19
ENSG00000244067	GSTA2	glutathione S-transferase alpha 2	177.9	50.98	−1.53	8.83E−18
ENSG00000129538	RNASE1	ribonuclease A family member 1, pancreatic	96.52	29.63	−1.38	1.60E−12
ENSG00000109084	TMEM97	transmembrane protein 97	30.27	11.17	−1.18	3.87E−12
ENSG00000135409	AMHR2	anti-Mullerian hormone receptor type 2	1.65	0.24	−2.7	3.47E−11
ENSG00000243955	GSTA1	glutathione S-transferase alpha 1	335.07	149.5	−1.18	3.84E−11
ENSG00000167183	PRR15L	proline rich 15 like	23.81	9.83	−1.24	3.84E−11
ENSG00000185176	AQP12B	aquaporin 12B	2.47	0.86	−2.5	3.84E−11
ENSG00000145703	IQGAP2	IQ motif containing GTPase-activating protein 2	12.55	6.99	−1.09	4.26E−11
ENSG00000187021	PNLIPRP1	pancreatic lipase related protein 1	145.68	34.43	−1.47	7.56E−11
ENSG00000103375	AQP8	aquaporin 8	7.88	0.69	−2.78	7.56E−11
ENSG00000169562	GJB1	gap junction protein beta 1	14.77	5.72	−1.11	1.19E−10
ENSG00000112394	SLC16A10	solute carrier family 16 member 10	2.48	1.06	−1.6	9.65E−10
ENSG00000090382	LYZ	lysozyme	567.11	356.85	−0.91	1.11E−9
ENSG00000165449	SLC16A9	solute carrier family 16 member 9	14.57	6.96	−0.98	1.14E−9
ENSG00000085276	MECOM	MDS1 and EVI1 complex locus	7.03	3.07	−1.06	1.26E−9
ENSG00000049246	PER3	period circadian regulator 3	13.72	7.26	−0.94	1.54E−9
ENSG00000101825	MXRA5	matrix remodeling associated 5	7.66	2.99	−1.06	1.61E−9

GTP, guanosine triphosphate; TGF-β, transforming growth factor β.
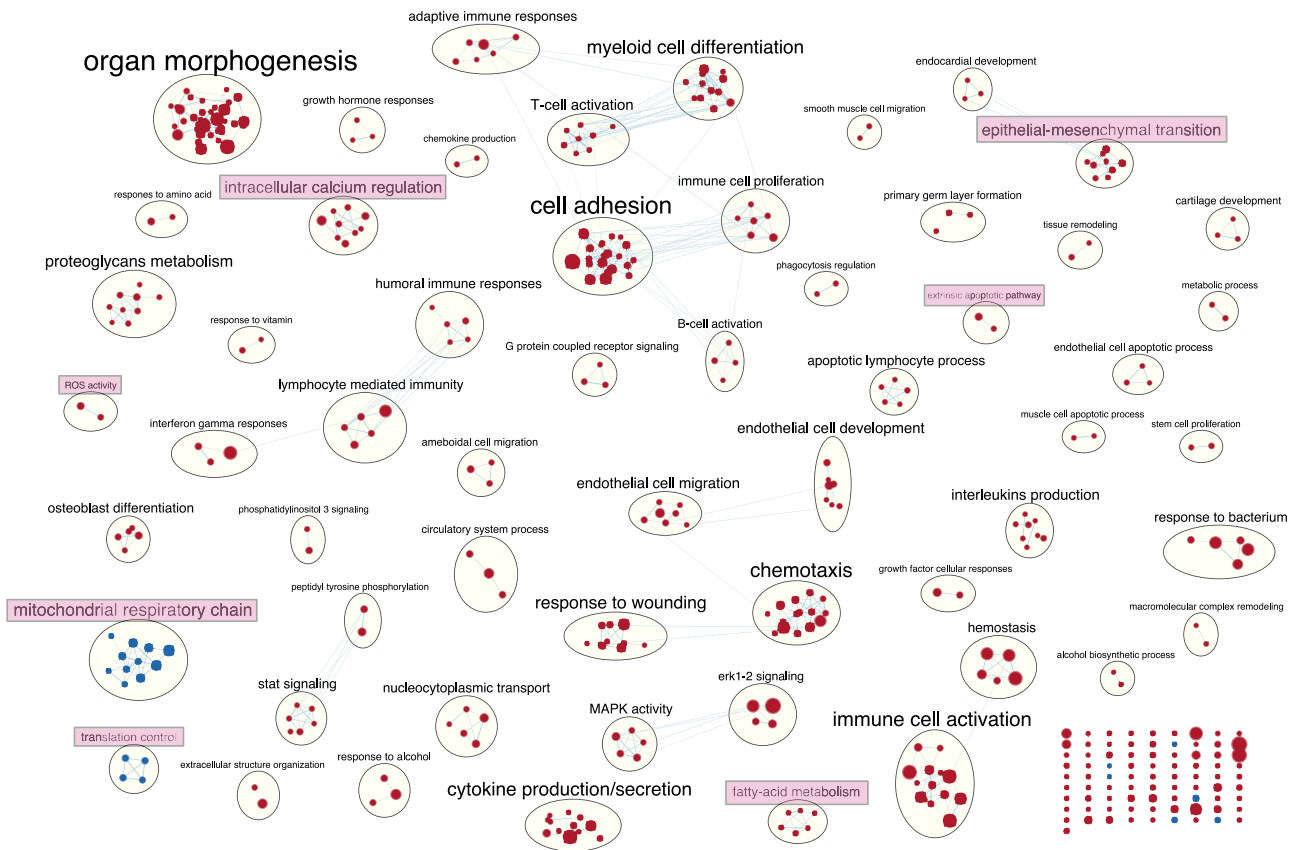
Figure 4. Enrichment Map Analysis of the Transcriptomic Differences between T2D and ND Islets
Red indicates upregulated and blue indicates downregulated processes.

forbidden) genes from earlier work (Pullen et al., 2010; Thorrez et al., 2011; Lemaire et al., 2017; Pullen et al., 2017), we selected 20 genes that were common to at least 2 of these studies. The expression of these genes plus 4 β cell dedifferentiation and 11 β cell identity markers (Diedisheim et al., 2018) was examined in the 3 treatments (P, G, and P+G) (Figure S3B). We found that 8 genes showed differential expression. Two disallowed genes, *IGFBP4* and *CAT*, were significantly upregulated by P and P+G, respectively. After washout, IGFBP4 induction was reversed. IGFBP4 is a member of the insulin-like growth factor binding protein family that is required for adipogenesis and influences fat depot distribution (Maridas et al., 2017). *CAT* encodes a peroxisomal, key antioxidant enzyme catalyzing hydrogen peroxide decomposition. *MYC*, encoding a nuclear phosphoprotein that plays a role in apoptosis (McMahon 2014) and cellular transformation (Gill et al., 2013), was upregulated by P+G and reverted to control levels after washout, suggesting transitory dedifferentiation. The β cell identity markers *MAFA*, *MAFB*, *PAX6*, and *SLC30A8* were significantly downregulated by P, and only MAFA reverted with washout. For P+G, *INSM1* was downregulated at D4. MAFA and MAFB are β cell transcription factors that regulate insulin gene expression (Olbrot et al., 2002) and β cell differentiation (Russell et al., 2020). INSM1 (insulinoma transcriptional repressor) is involved in endocrine

pancreas differentiation (Osipovich et al., 2014). The transcription factor PAX6 is required for the maintenance of β cell identity and function (Swisa et al., 2017a). In summary, lipotoxic conditions with or without the concurrent high glucose caused β cell dedifferentiation, while high glucose per se did not.

Validation Studies of Selected Genes
To confirm the presence and role of genes affected by the lipoglucotoxic incubations, we performed several validation experiments. Islets from 3 ND donors were studied by shotgun proteomics 2 days after isolation to evaluate the expression of proteins corresponding to the top dysregulated genes in P-washed-out islets (D8 washout) versus P-exposed islets (D4) (Table 1). The proteins identified by mass spectrometry (MS) (only proteins expressed in at least two of the three preparations were considered) are reported in Table S3, together with some of the parameters related to their identification. Examples of peptide MS/MS spectra are provided in Data S2. These results confirm that human islets express proteins coded by genes that are affected by P-exposure and washout. However, we did not study islet proteomics changes over the time in control and lipoglucotoxicity conditions.

One of the upregulated genes associated with improved β cell function in D8 washout versus D4 P- treated islets was

ANKRD23 (Table S2B). *ANKRD23* is a nuclear transcriptional regulatory protein that downregulates the expression of LKB1, an activator of AMP-activated protein kinase (AMPK) (Shimoda et al., 2015; Sun et al., 2015). *ANKRD23* is downregulated in T2D islets and β cells (Solimena et al., 2018; Marselli et al., 2010). When we overexpressed *ANKRD23* in MIN6B1 cells (Miyazaki et al., 1990) (Figure S5Aa), AMPK phosphorylation at T172 of the catalytic alpha subunit (pAMPK) tended to increase at g (3.0 mmol/L) (Figure S5Ab). Phosphorylation of the downstream AMPK substrates pRaptor and pACC (acetyl-CoA carboxylase) also tended to increase (Figure S5Ac and d). Consequently, in *ANKRD23*-transfected cells, G (30 mmol/L) led to a significant change in pRaptor (Figure S5Ac). These data suggest that *ANKRD23* induction during the recovery of P-treated islets affects AMPK activity, with resultant improvement in GSIS (Rutter et al., 2015; Fu et al., 2013).

We also investigated the role of *SEC61G*, which was upregulated in the P+G-exposed human islets (Table S2E). This gene encodes the gamma subunit of the protein translocation apparatus in the ER membrane (Linxweiler et al., 2017). ER stress induces *SEC61G* expression, and *SEC61G* silencing causes apoptosis (Lu et al., 2009). We performed experiments with rat INS-1E cells, human EndoC-βH1 cells, and dispersed human islet cells, finding that P and thapsigargin increased the expression of SEC61G (Figure S5Ba). Silencing of Sec61G/SEC61G (Figure S5Bb–d) induced β cell apoptosis, assessed by staining with nuclear dyes (Figure S5Be–g) and caspase 3 and 9 cleavage (Figure S5Bh).

Association with T2D Genome-wide Association Loci

To investigate whether genes associated with T2D by genome-wide association studies (GWASs) were influenced by the lipoglucotoxic environments, we analyzed their overlap with dysregulated islet genes in the P and P+G conditions (Figure 1). We included >400 *loci* associated with T2D and related traits reported in the GWAS catalog (http://www.ebi.ac.uk/gwas) and a recently published study (Mahajan et al., 2018). We found 63 overlapping genes (Table S4A), corresponding to ∼15% of the total T2D and associated trait *loci*. Of these, 32 were dysregulated by P (12 upregulated and 20 downregulated) and 43 by P+G (18 upregulated and 25 downregulated). Twelve genes were dysregulated in both stress conditions, with a consistent direction of effect. Interestingly, 7 genes that were modified by P at D4 recovered after washout, namely *ACSL1*, a gene that activates fatty acids for lipid metabolism (Kycia et al., 2018; Li et al., 2006), *FADS1* and *FADS2*, fatty acid desaturases involved in polyunsaturated fatty acid synthesis (Lytrivi et al., 2020), and the transmembrane protein *TMEM154*, variants that associate with β cell dysfunction (Harder et al., 2015). *C2CD4A* and *C2CD4B*, which are involved in calcium ion exocytosis and vesicle fusion, recovered in both P and P+G washed-out islets. The *C2CD4A/C2CD4B* locus is associated with glucose-stimulated insulin response (Grarup et al., 2011). Consistent with our observations, this locus is located in an islet-specific enhancer, and the risk variant increases both *C2CD4A* and *C2CD4B* expression (Kycia et al., 2018). In agreement with our insulin secretion data, we found that more of these key genes recovered after palmitate alone (n = 7) compared to P+G (n = 3) washout.

To obtain further biological insight into the causal role of GWAS genes, we compared dysregulated genes with our recently published catalog of cis-expression quantitative trait *loci* (cis-eQTL) performed in human islets (Khamis et al., 2019). We found that 16 dysregulated genes in P- and P+G-treated islets had an eQTL, 62% of which did not implicate the gene reported by GWAS (Table S4B). Seven of these genes were consistent in the direction of effect for the risk allele in eQTL and response to treatment. Interestingly, among the genes that were found in both lipoglucotoxic experiments, *WARS* and *PDE8B* have previously been reported as having an eQTL (van de Bunt et al., 2015; Viñuela et al., 2020). P and P+G treatments also showed specific eQTLs in *ADCY5*, an adenylate cyclase family member involved in insulin secretion (Hodson et al., 2014). eQTLs in *ATP2A3*, encoding the ER Ca²⁺ pump SERCA3, were unique for P-treated islets, and, conversely, *HKDC1*, *UBE2Z*, and *PHLDA2* eQTLs were unique to P+G-treated islets. Interestingly, knockout of *HKDC1* in mice has revealed its role in glucose homeostasis (Ludvik et al., 2016). The role of *UBE2Z* in β cell biology and diabetes has not yet been established. In turn, *KCNQ1* was the reported GWAS gene for *PHLDA2* and this *locus* has been found to be robustly associated with T2D (Sun et al., 2012).

These results demonstrate that a proportion of genes significantly affected by lipoglucotoxicity have an eQTL and that the effects of genes that were implicated in T2D and associated traits had an eQTL persisting after washout for both P and P+G conditions.

T2D versus ND Human Islet Transcriptomes

We next analyzed T2D human islet function and gene expression signature. As expected, insulin release in response to acute stimulation by different secretagogues was lower from T2D islets (Figure S6), confirming previous findings (Deng et al., 2004; Del Guerra et al., 2005; Solimena et al., 2018). RNA-seq was performed on islets isolated from 28 T2D and 58 ND donors (Table S1). After Benjamini-Hochberg correction for multiple comparisons, 152 genes were differentially expressed in T2D versus ND islets (72 upregulated and 80 downregulated; Table S5A). Previous work has evaluated human T2D islet gene expression by microarray analysis (Gunton et al., 2005; Taneera et al., 2012; Bugliani et al., 2013; Solimena et al., 2018). The present study has used RNA-seq analysis to compare the transcriptomes of large T2D and ND islet series.

Gene sets were organized into networks by Enrichment Map, as was done for the lipoglucotoxic conditions. This analysis showed the upregulation of fatty acid metabolism, intracellular calcium regulation, reactive oxygen species processing, and the downregulation of mitochondrial respiratory chain, and translational control (Figure 4). The gene sets and individual genes comprising these categories are reported in Data S1D, showing several similarities with those observed in glucotoxic and/or lipotoxic experiments.

Comparison of Lipoglucotoxic and T2D Islet Gene Expression Signatures by Rank-Rank Hypergeometric Overlap (RRHO)

RRHO allows us to compare differentially expressed transcriptomes between independent experiments in a threshold-free
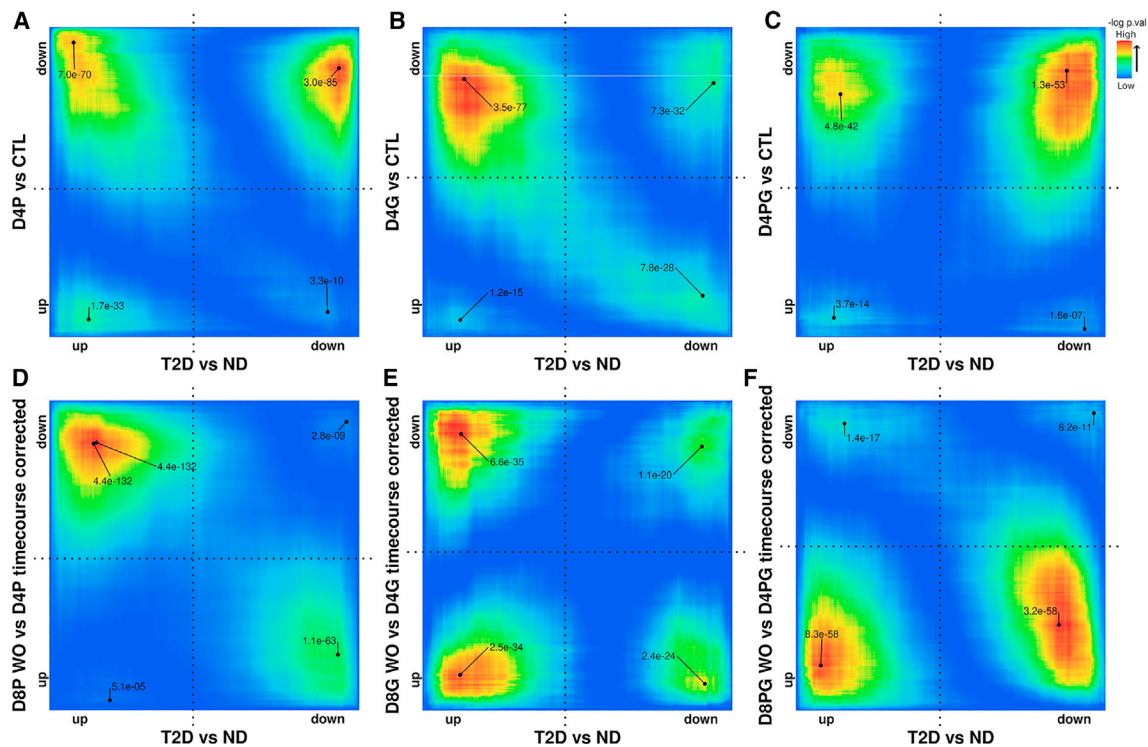
Figure 5. RRHO Map Showing Overlaps between Transcriptome Comparisons

Differential expression of T2D versus ND islets were compared with differential expression of:

(A) D4 P-exposed versus D4 controls.

(B) D4 G-exposed versus D4 controls.

(C) D4 P+G-exposed versus D4 controls.

(D) D8 P washed-out versus D4 P-exposed islets.

(E) D8 G washed-out versus D4 G-exposed islets.

(F) D8 P+G washed-out versus D4 P+G-exposed islets.

Genes are ranked by fold change from most downregulated to most upregulated. The level map colors show −log p values for overlap, with an indication of the smallest p value for clusters with statistically significant overlap between genes upregulated in both datasets (bottom left quadrant), downregulated in both (top right quadrant), upregulated in T2D and down in lipotoxic/glucotoxic conditions (top left quadrant), and downregulated in T2D and upregulated by lipotoxicity/ glucotoxicity (bottom right quadrant). The RRHO method is further described in Figure S7 with 4 illustrative level maps.

manner and visualize the significance and direction of the overlap (Plaisier et al., 2010). In Figure S7, examples of RRHO maps are shown for different theoretical scenarios. The absence of overlap between 2 random transcriptome datasets, X and Y, is indicated by the blue color (Figure S7A); identical gene expression changes in datasets X and Y generate perfect overlap indicated by the red color (Figure S7B); identical, correlated, or anticorrelated gene expression changes among the top upregulated or downregulated genes in the 2 datasets generate a strong signal in the respective quadrants (Figures S7C and S7D).

We used the RRHO tool to compare the transcriptomes of islets from T2D versus ND donors with those of D4 P versus the respective D4 control islets (Figure 5A). There was significant overlap, particularly in genes upregulated in T2D versus ND and downregulated in D4 P versus control (n = 231) and also in genes upregulated (n = 246) or downregulated (n = 396) in both series (Figure 5A). The respective genes, processes, and pathways are listed in Tables S5B–S5D. The oppositely regulated genes belonged to inflammatory/immunological responses, indi-

cating a more profound involvement of T2D islets in such processes (Table S5B). The concordantly upregulated genes belonged to peroxisome proliferator-activated receptor (PPAR) signaling, inflammatory, and protein secretion pathways (Table S5C). Among the genes concordantly downregulated (Table S5D), there were several key regulators of β cell function and identity and/or genes previously found to be downregulated in T2D islets, such as *SLC2A2*, *MAFA*, *PDX1*, *CHL1*, and *FFAR4* (Fadista et al., 2014; Ganic et al., 2016; Solimena et al., 2018). In agreement with the functional results showing impaired insulin release in both P-exposed (Figure 2) and T2D islets (Figure S6), the commonly downregulated genes were essentially associated with β cell insulin secretion (Table S5D).

D4 high glucose exposure was mostly anticorrelated with the transcriptomes of T2D versus ND islets (Figure 5B), with 690 genes upregulated in T2D and downregulated by high glucose. Functional enrichment for these genes again revealed enriched pathways of inflammatory and immune responses (Table S5E), pointing to a more "inflamed" status of the diabetic islets.

The addition of high glucose to the fatty acid was associated at D4 with the RRHO pattern illustrated in Figure 5C. There were 783 overlapping genes upregulated in T2D versus ND and downregulated in lipoglucotoxicity-exposed islets, again mainly identifying inflammation-associated pathways (Table S5F). There was an exacerbated overlap in genes downregulated in both series (n = 559), essentially associated with metabolic processes (Table S5G). Fewer genes were upregulated in both T2D versus ND and P+G-treated versus control islets, or downregulated in the former and upregulated in the latter (Figure 5C).

The anticorrelated inflammatory/immune responses observed in T2D (up) and lipoglucotoxic conditions (down) is most likely the result of *in vivo* recruitment of immune cells to islets in T2D (Lytrivi et al., 2018). The T2D islet transcriptomes are enriched for macrophage and other immune cell signatures (Nirmal et al., 2018), while the three *ex vivo* lipoglucotoxic exposures decreased the expression of macrophage and monocyte genes (Data S1E).

Next, we compared the transcriptomes of T2D versus ND islets with those of D8 islets exposed to palmitate and then washed out (with recovered GSIS) versus D4 P-exposed islets (with impaired GSIS), showing a distinct scenario (Figure 5D). A marked reduction in concordant genes and an increase in anticorrelated genes was seen in this RRHO, in keeping with the recovered GSIS after P washout. There were 772 genes upregulated in T2D versus ND and downregulated in the washed-out islets; these again belonged to inflammatory and immune responses, confirming the more "inflamed" status of the diabetic islets, and extracellular matrix organization (Table S5H). Significant overlap was also seen for 430 genes that were downregulated in T2D versus ND and upregulated in the P washout islets; these genes were essentially associated with the β cell molecular phenotype and insulin secretion (Table S5I).

The transcriptomes of T2D versus ND islets were then compared with those of D8 islets exposed to G and then washed out (with recovered GSIS) versus D4 high glucose-exposed islets (with impaired GSIS), showing a distinct scenario (Figure 5E). There was significant overlap of a total of 395 genes upregulated in T2D versus ND and downregulated in D8 high glucose washout (Table S5J). Functional enrichment for these genes identified regulation of immune response and calcium ion homeostasis. There was also significant overlap of 396 genes upregulated in both T2D versus ND and D8 G versus D4 G, pertaining to enrichment of immune system and inflammatory response (Table S5K). The 370 genes downregulated in both conditions were related to calcium ion-dependent exocytosis and β cell development (Table S5L), while the 238 genes downregulated in T2D and upregulated in high glucose washout were related to hypoxia (Table S5M).

Figure 5F illustrates the RRHO for T2D versus ND islets compared to islets previously cultured with P+G versus the islets after P+G washout (with no functional recovery). Again, many genes (n = 311) were upregulated in T2D versus ND and downregulated in the washed-out islets (D8) versus P+G-exposed islets (D4) that were associated with extracellular matrix organization and inflammatory responses (Table S5N). There was also a large and highly significant enrichment in genes (n = 410) upregulated in both washout and T2D islets that identified additional inflammation processes (Table S5O). Intriguingly, genes upregulated in D8 washed-out P+G islets and downregulated in T2D versus ND pertained to insulin secretion and regulation thereof (Table S5P). A few key β cell genes, such as *PDX1*, or pathways associated with β cell identity, were not affected by the washout.

These RRHO analyses showed that persistent or transient human β cell dysfunction induced by metabolic stress was accompanied by specific gene expression signatures that are shared with T2D, with the greatest concordant overlap between conditions that induce β cell dysfunction and fail to recover after washout.

DISCUSSION

The present study provides comprehensive information on the functional and molecular changes associated with β cell damage and rescue in human islets exposed to lipo- and/or glucotoxicity in human islets. Furthermore, it shows that persistent or transient GSIS dysfunction induced by metabolic stress associates with specific traits and shared gene expression of T2D islets.

To ensure relevance to human disease and augment translational potential, we used human islets for all key experiments, after carefully standardizing and validating procedures for islet isolation, *ex vivo* culture, functional assessment, ultrastructural examination and molecular analyses, as described in our previous studies (Marchetti et al., 2007; ; Cunha et al., 2009·Masini et al., 2009; Cnop et al., 2014; Oliveira et al., 2015; Khamis et al., 2019). By doing so, we avoided many of the limitations inherently associated with the use of different experimental models, including species differences and variation in *ex vivo* and *in vivo* experimental protocols (Hart and Powers, 2019; Poitout et al., 2019; Marchetti et al., 2019).

We showed that several, but not all, of the tested metabolic stresses had direct deleterious effects on human β cell insulin secretion, depending on the type and concentration of the stressors and their combinations and indicating that β cells effectively cope with "mild," temporary metabolic stress. More important, we observed that GSIS defects were largely corrected by 4-day culture in "normal" (i.e., 5.5 mmol/L glucose-containing) medium for islets previously exposed to 0.5 mmol/L P alone or in combination with 11.1 mmol/L g, and confirmed previous data showing functional recovery of human islets exposed to 22.2 mmol/L G glucotoxicity (Davalli et al, 1991; Eizirik et al., 1992; Marshak et al., 1999). Thus, under certain conditions, β cell dysfunction is not irreversible but can be rescued. Our *ex vivo* exposure to the metabolic insults was short term (2 days). The impact of longer-term lipoglucotoxicity was assessed *in vivo* by transplanting human islets into immunodeficient mice subsequently fed a high-fat diet, treated with the insulin receptor antagonist S961, or undergoing mouse β cell ablation (Gargani et al., 2013; Dai et al., 2016). These experiments showed that lipoglucotoxicity induced human β cell dysfunction, but the transcriptome signatures of the metabolic insults (and possible recovery) were not examined. *In vivo* work in humans has shown that alleviating the metabolic burden induced by lipotoxicity or glucotoxicity or obesity leads to improved insulin secretion (Paolisso et al., 1995; Kashyap et al., 2003; Cusi et al., 2007; Solomon et al., 2012; Camastra

et al., 2013; Mingrone et al., 2015; White et al., 2016; Steven et al., 2016; Taylor et al., 2018; Lean et al., 2018). Therefore, the functional results of the present study support the use of human islets exposed to metabolic stresses as a valid model to gain insights on the *in vivo* pathophysiology of β cell dysfunction.

Functional recovery was not observed, however, with islets that had been cultured with 0.5 mmol/L P plus 22.2 mmol/L G, or 1.0 mmol/L P+O plus 22.2 mmol/L G. The combination of P+G was associated with persistent β cell dysfunction even after removal of the toxic insult, which may contribute to the progressive deterioration of β cell function in T2D patients (UK Prospective Diabetes Study [UKPDS] Group, 1998; Weir et al., 2009) and the lack of T2D remission in a proportion of subjects after bariatric surgery or a very-low-calorie diet (Camastra et al., 2013; Mingrone et al., 2015; Taylor et al., 2018, 2019; Lean et al., 2018). Our results suggest that lack of reversibility of the induced β cell damage should also be taken into consideration when defining a condition as lipotoxic and/or glucotoxic.

To understand the molecular mechanisms behind our present observations, we performed extensive time course transcriptome analyses by RNA-seq to map molecular events underlying the impairment of glucose-stimulated insulin secretion and its persistence or recovery, induced by, respectively, exposure to P alone or P+G. The complex adaptive transcriptome modifications of human islets exposed to P included increased fatty acid metabolism and unfolded protein response, as well as reduced cell adhesion/activation, cell proliferation, neuronal differentiation, and organ morphogenesis. We also identified a gene expression signature consistent with β cell dedifferentiation, with the acquisition of disallowed gene expression and loss of β cell identity markers. Overall, these findings are in line with previous data obtained by RNA-seq or microarrays (Cnop et al., 2014; Hall et al., 2014).

A major finding of the present study is the observation that the recovery of GSIS from human islets after P washout was associated with specific transcriptomic changes. A few studies have described the interplay between fatty acid and glucose metabolism in β cells under lipotoxic stress (Shuldiner and McLenithan, 2004; Poitout and Robertson, 2008; Cunha et al., 2008; Janikiewicz et al., 2015), and the underlying biochemical mechanisms and the reciprocal relationships have been reviewed recently (Lytrivi et al., 2020). Here, we show that the functional recovery of P-exposed human islets was accompanied by the downregulation of fatty acid metabolism and the upregulation of carbohydrate catabolism pathways. As for this latter process, two genes in particular were upregulated, namely *AK2* (adenylate kinase 2) and *PGAM2* (phosphoglycerate mutase). AK2 is localized in the mitochondrial intermembrane space and is involved in the regulation of adenine nucleotide composition. AK2 deficiency impairs mitochondrial function and oxidative phosphorylation (Six et al., 2015). In β cells, AK2 also interacts with AMPK to modulate K_{ATP} channel function (Beall et al., 2013). *PGAM2* encodes a glycolytic enzyme that catalyzes the reversible conversion of 3-phosphoglycerate into 2-phosphoglycerate in glycolysis (Fothergill-Gilmore and Watson, 1989). The overexpression of *Pgam2* in the mouse heart (reminiscent of the effects of recovery from lipotoxicity in the present study) changed the levels of key intermediates, including an increase

in its substrates and products 3-phosphoglycerate (3-PG) and 2-PG (Okuda et al., 2013). Both 3-PG and 2-PG are allosteric regulators: 3-PG inhibits 6-phosphogluconate dehydrogenase in the pentose phosphate pathway, whereas 2-PG activates phosphoglycerate dehydrogenase (PHGDH), which is involved in glycine and serine synthesis (Hitosugi et al., 2012). The results from the study by Okuda et al. (2013) should be interpreted with caution, however, as the degree of overexpression of the protein (10-fold above the endogenous level) was substantial and affected the expression of other glycolytic and respiratory chain enzymes. Further studies are therefore needed to better determine the role of PGAM2 on β cell energy balance.

The combination of P+G (a condition to which islets of T2D individuals may be exposed for years) (Weir et al., 2009; Chatterjee et al., 2017; Lascar et al., 2018) induced even greater (2-fold more) modifications in the human islet transcriptome. The upregulated biological processes included unfolded protein response, protein degradation, immune surface receptor, autophagy, ER stress-induced and extrinsic apoptotic pathways, mRNA splicing regulation, and nuclear transport. In keeping with the persistent impairment of GSIS after washout (D8), the expression of the majority of these genes (76%) remained unchanged, as compared to D4 lipoglucotoxicity-exposed islets. We cannot exclude that more favorable changes may occur with longer washout. However, our data indicate that a severely dysmetabolic environment can lead to β cell alterations that are difficult to rescue. This could explain why ~30%–50% of T2D patients do not demonstrate diabetes remission after bariatric surgery or a very-low-calorie diet (Sjöström et al., 2004; Mingrone et al., 2015; White et al., 2016; Taylor et al., 2018). It also implies the need for "aggressive" glucose- and lipid-lowering therapy as early as possible in the natural history of T2D (Kramer et al., 2013; Davies et al., 2018) to preserve functional β cell mass.

On top of this, our comprehensive genomics analysis further supports the functional and transcriptomic effects. For many GWAS and eQTL genes, the genetic effects manifested through altered expression in response to lipoglucotoxicity, providing interesting insights into the causal relationship of these variants. We found that the effects of some of these genes persisted after washout, pointing to long-term consequences of lipotoxicity and glucotoxicity. An interesting finding was the detection of candidate genes involved in fatty acid and lipid metabolism, such as *ACSL1*, *FADS1*, and *FADS2*. We also found that many monogenic diabetes genes were dysregulated by metabolic stress, including genes that cause permanent neonatal diabetes (*PDX1*, *INS*, and *MNX1*) (Bonnefond et al., 2014; De Franco et al., 2013; Støy et al., 2007) in the case of P treatment, and maturity-onset diabetes of the young (*HNF4A* and *HNF1B*) (Chandra et al., 2013; Furuta et al., 1997) for P+G treatment. *Ex vivo* lipoglucotoxic treatments of human islets are hence a valuable tool for investigating diabetes candidate genes.

Another strength of this study is the RNA-seq analysis of a large series of T2D islets. It identified a wealth of T2D gene-set signatures. Fadista et al. (2014) reported on islet transcriptomes of 51 normoglycemic, 15 impaired glucose tolerant, and 12 diabetic donors. More recently, Viñuela et al. (2020) used previously published datasets (Nica et al., 2013; Fadista

et al., 2014; van de Bunt et al., 2015; Varshney et al., 2017) and newly collected samples to determine the effects of genetic variants on the transcriptome of human islets (including 37 T2D samples). Whereas experimental differences make a direct comparison of such data with the present results difficult, our approach allowed us to compare potential overlap by RRHO between transcriptomes of T2D versus ND islets with those of islets undergoing or recovering from lipotoxicity or lipoglucotoxicity. At the molecular level, T2D islets have a more marked inflammatory status compared to islets exposed to lipotoxicity. The occurrence of inflammation in T2D islets has been previously demonstrated histologically (Marselli et al., 2013; Donath et al., 2013; Marchetti, 2016; Eguchi and Nagai, 2017). Interestingly, an anticorrelation with the T2D versus ND pattern was seen after P washout, with the upregulation of several genes and pathways associated with β cell function and identity for D8 P washout versus D4 P. Among such genes, *SMAD9*, *TLE6*, *TSPAN1*, *TTC39C*, *PDLIM2*, *PLAGL1*, *GREM2*, *CHODL*, and *ID1* ranked among the 20 most upregulated genes in the comparison of D8 versus D4. With the exception of *PLAGL1*, which is associated with neonatal diabetes (Touati et al., 2019), and *ID1*, a helix-loop-helix protein that negatively regulates β cell function and differentiation in lipotoxic conditions (Akerfeldt and Laybutt, 2011), the other genes (*SMAD9*, involved in transforming growth factor β [TGF-β] signaling; *TLE6*, a transcriptional co-repressor; *TSPAN1*, a transmembrane protein; *TTC39C*, a broadly expressed gene of uncertain function; *PDLIM2*, associated with cell migration and adhesion; *GREM2*, playing a role in regulating organogenesis; and *CHODL*, a type I membrane protein with a carbohydrate recognition domain for certain lectins) have not been associated with T2D and/or insulin secretion so far. These genes are associated with rescued β cell function and may hence represent potential targets for β cell specifically directed therapies.

Exposure to P+G drove changes in the islet transcriptome indicative of inflammatory responses even after metabolic stress removal that overlapped with those of T2D islets. Although some functional pathways recovered after the removal of the lipoglucotoxic insult, GSIS remained impaired after washout. This was probably related to the persistent inhibition of some genes that are key for the maintenance of the differentiated β cell phenotype (e.g., PDX1, GCK, which is lost in conditions of metabolic stress and in T2D) (Rutter et al., 2015; Cinti et al., 2016; Swisa et al., 2017b; Marchetti et al., 2017; Bensellam et al., 2018).

Therefore, lipotoxicity may favor the onset of T2D by interfering with mechanisms controlling β cell function that can be rescued; the addition of a second layer of metabolic stress (e.g., in the P+G exposure) may contribute to the progression of disease through more profound and potentially irreversible molecular alterations.

In conclusion, this study identifies mechanisms responsible for the deterioration and recovery of human β cell function under metabolic stress, and points to significant overlap with T2D islet molecular traits. Whereas islet single-cell work, with its exciting challenges (Wang and Kaestner, 2019), will likely provide further information on these issues in the future, our insights into T2D islet pathophysiology can foster the development of improved β cell targeted therapeutic strategies.

STAR★METHODS

Detailed methods are provided in the online version of this paper and include the following:

- KEY RESOURCES TABLE
- RESOURCE AVAILABILITY
  - Lead Contact
  - Materials Availability
  - Data and Code Availability
- EXPERIMENTAL MODEL AND SUBJECT DETAILS
  - Human pancreatic islets
  - Cell lines
- METHOD DETAILS
  - Human pancreatic islet lipoglucotoxic stress conditions and washout
  - Insulin secretion studies
  - Immunocytochemistry and electron microscopy
  - RNA extraction and library preparation from the islets
  - Validation studies: Proteomics experiments
  - Validation studies: ANKRD23 experiments
  - Validation studies: Sec61G experiments
- QUANTIFICATION AND STATISTICAL ANALYSIS
  - RNA-seq data analysis
  - Evaluation of functional enrichment
  - Proteomic data analysis
  - Expression quantitative trait loci (eQTL) analysis
  - Statistical analysis

SUPPLEMENTAL INFORMATION

Supplemental Information can be found online at https://doi.org/10.1016/j.celrep.2020.108466.

AUTHOR CONTRIBUTIONS

Conceptualization, L.M., M. Suleiman, A. Pocai, L.N., D.L.E., M. Cnop, and P.M.; Methodology, L.M., A. Piron, M. Suleiman, M.I., M. Cnop, and P.M.;

REFERENCES

Accili, D., Talchai, S.C., Kim-Muller, J.Y., Cinti, F., Ishida, E., Ordelheide, A.M., Kuo, T., Fan, J., and Son, J. (2016). When β-cells fail: lessons from dedifferentiation. Diabetes Obes. Metab. *18* (*Suppl 1*), 117–122.

Akerfeldt, M.C., and Laybutt, D.R. (2011). Inhibition of Id1 augments insulin secretion and protects against high-fat diet-induced glucose intolerance. Diabetes *60*, 2506–2514.

Asfari, M., Janjic, D., Meda, P., Li, G., Halban, P.A., and Wollheim, C.B. (1992). Establishment of 2-mercaptoethanol-dependent differentiated insulin-secreting cell lines. Endocrinology *130*, 167–178.

Ashcroft, F.M., and Rorsman, P. (2012). Diabetes mellitus and the β cell: the last ten years. Cell *148*, 1160–1171.

Beall, C., Watterson, K.R., McCrimmon, R.J., and Ashford, M.L. (2013). AMPK modulates glucose-sensing in insulin-secreting cells by altered phosphotransfer to KATP channels. J. Bioenerg. Biomembr. *45*, 229–241.

Benjamini, Y., and Hochberg, Y. (1995). Controlling the False Discovery Rate: a practical and powerful approach to multiple testing. J. R. Stat. Soc. Ser. B. *1*, 289–300.

Benjamini, Y., and Yekutieli, D. (2001). The control of the false discovery rate in multiple testing under dependency. Ann. Stat. *29*, 1165–1188.

Bensellam, M., Jonas, J.C., and Laybutt, D.R. (2018). Mechanisms of β-cell dedifferentiation in diabetes: recent findings and future research directions. J Endocrinol *236*, R109–R143.

Bensellam, M., Laybutt, D.R., and Jonas, J.C. (2012). The molecular mechanisms of pancreatic β-cell glucotoxicity: recent findings and future research directions. Mol. Cell. Endocrinol. *364*, 1–27.

Bonnefond, A., Philippe, J., Durand, E., Muller, J., Saeed, S., Arslan, M., Martínez, R., De Graeve, F., Dhennin, V., Rabearivelo, I., et al. (2014). Highly sensitive diagnosis of 43 monogenic forms of diabetes or obesity through one-step PCR-based enrichment in combination with next-generation sequencing. Diabetes Care *37*, 460–467.

Brozzi, F., Nardelli, T.R., Lopes, M., Millard, I., Barthson, J., Igoillo-Esteve, M., Grieco, F.A., Villate, O., Oliveira, J.M., Casimir, M., et al. (2015). Cytokines induce endoplasmic reticulum stress in human, rat and mouse beta cells via different mechanisms. Diabetologia *58*, 2307–2316.

Bugliani, M., Liechti, R., Cheon, H., Suleiman, M., Marselli, L., Kirkpatrick, C., Filipponi, F., Boggi, U., Xenarios, I., Syed, F., et al. (2013). Microarray analysis of isolated human islet transcriptome in type 2 diabetes and the role of the ubiquitin-proteasome system in pancreatic β cell dysfunction. Mol. Cell. Endocrinol. *367*, 1–10.

Cahill, K.M., Huo, Z., Tseng, G.C., Logan, R.W., and Seney, M.L. (2018). Improved identification of concordant and discordant gene expression signatures using an updated rank-rank hypergeometric overlap approach. Sci. Rep. *8*, 9588.

Camastra, S., Muscelli, E., Gastaldelli, A., Holst, J.J., Astiarraga, B., Baldi, S., Nannipieri, M., Ciociaro, D., Anselmino, M., Mari, A., and Ferrannini, E. (2013). Long-term effects of bariatric surgery on meal disposal and β-cell function in diabetic and nondiabetic patients. Diabetes *62*, 3709–3717.

Cardozo, A.K., Ortis, F., Storling, J., Feng, Y.M., Rasschaert, J., Tonnesen, M., Van Eylen, F., Mandrup-Poulsen, T., Herchuelz, A., and Eizirik, D.L. (2005). Cytokines downregulate the sarcoendoplasmic reticulum pump Ca2+ ATPase 2b and deplete endoplasmic reticulum Ca2+, leading to induction of endoplasmic reticulum stress in pancreatic beta-cells. Diabetes *54*, 452–461.

Chandra, V., Huang, P., Potluri, N., Wu, D., Kim, Y., and Rastinejad, F. (2013). Multidomain integration in the structure of the HNF-4α nuclear receptor complex. Nature *495*, 394–398.

Chatterjee, S., Khunti, K., and Davies, M.J. (2017). Type 2 diabetes. Lancet *389*, 2239–2251.

Cinti, F., Bouchi, R., Kim-Muller, J.Y., Ohmura, Y., Sandoval, P.R., Masini, M., Marselli, L., Suleiman, M., Ratner, L.E., Marchetti, P., and Accili, D. (2016). Evidence of β-Cell Dedifferentiation in Human Type 2 Diabetes. J. Clin. Endocrinol. Metab. *101*, 1044–1054.

Ciregia, F., Bugliani, M., Ronci, M., Giusti, L., Boldrini, C., Mazzoni, M.R., Mossuto, S., Grano, F., Cnop, M., Marselli, L., et al. (2017). Palmitate-induced lipotoxicity alters acetylation of multiple proteins in clonal β cells and human pancreatic islets. Sci. Rep. *7*, 13445.

Cnop, M., Hannaert, J.C., Hoorens, A., Eizirik, D.L., and Pipeleers, D.G. (2001). Inverse relationship between cytotoxicity of free fatty acids in pancreatic islet cells and cellular triglyceride accumulation. Diabetes *50*, 1771–1777.

Cnop, M., Welsh, N., Jonas, J.C., Jörns, A., Lenzen, S., and Eizirik, D.L. (2005). Mechanisms of pancreatic beta-cell death in type 1 and type 2 diabetes: many differences, few similarities. Diabetes *54* (*Suppl 2*), S97–S107.

Cnop, M., Ladriere, L., Hekerman, P., Ortis, F., Cardozo, A.K., Dogusan, Z., Flamez, D., Boyce, M., Yuan, J., and Eizirik, D.L. (2007). Selective inhibition of eukaryotic translation initiation factor 2 alpha dephosphorylation potentiates fatty acid-induced endoplasmic reticulum stress and causes pancreatic beta-cell dysfunction and apoptosis. J. Biol. Chem. *282*, 3989–3997.

Cnop, M., Abdulkarim, B., Bottu, G., Cunha, D.A., Igoillo-Esteve, M., Masini, M., Turatsinze, J.V., Griebel, T., Villate, O., Santin, I., et al. (2014). RNA sequencing identifies dysregulation of the human pancreatic islet transcriptome by the saturated fatty acid palmitate. Diabetes *63*, 1978–1993.

Coomans de Brachène, A., Dos Santos, R.S., Marroqui, L., Colli, M.L., Marselli, L., Mirmira, R.G., Marchetti, P., and Eizirik, D.L. (2018). IFN-α induces a preferential long-lasting expression of MHC class I in human pancreatic beta cells. Diabetologia *61*, 636–640.

Cunha, D.A., Hekerman, P., Ladrière, L., Bazarra-Castro, A., Ortis, F., Wakeham, M.C., Moore, F., Rasschaert, J., Cardozo, A.K., Bellomo, E., et al. (2008). Initiation and execution of lipotoxic ER stress in pancreatic beta-cells. J. Cell Sci. *121*, 2308–2318.

Cunha, D.A., Ladrière, L., Ortis, F., Igoillo-Esteve, M., Gurzov, E.N., Lupi, R., Marchetti, P., Eizirik, D.L., and Cnop, M. (2009). Glucagon-like peptide-1 agonists protect pancreatic beta-cells from lipotoxic endoplasmic reticulum stress through upregulation of BiP and JunB. Diabetes *58*, 2851–2862.

Cusi, K., Kashyap, S., Gastaldelli, A., Bajaj, M., and Cersosimo, E. (2007). Effects on insulin secretion and insulin action of a 48-h reduction of plasma free fatty acids with acipimox in nondiabetic subjects genetically predisposed to type 2 diabetes. Am. J. Physiol. Endocrinol. Metab. *292*, E1775–E1781.

Dai, C., Kayton, N.S., Shostak, A., Poffenberger, G., Cyphert, H.A., Aramandla, R., Thompson, C., Papagiannis, I.G., Emfinger, C., Shiota, M., et al. (2016). Stress-impaired transcription factor expression and insulin secretion in transplanted human islets. J. Clin. Invest. *126*, 1857–1870.

Davalli, A.M., Ricordi, C., Socci, C., Braghi, S., Bertuzzi, F., Fattor, B., Di Carlo, V., Pontiroli, A.E., and Pozza, G. (1991). Abnormal sensitivity to glucose of human islets cultured in a high glucose medium: partial reversibility after an additional culture in a normal glucose medium. J. Clin. Endocrinol. Metab. *72*, 202–208.

Davies, M.J., D'Alessio, D.A., Fradkin, J., Kernan, W.N., Mathieu, C., Mingrone, G., Rossing, P., Tsapas, A., Wexler, D.J., and Buse, J.B. (2018). Management of hyperglycaemia in type 2 diabetes, 2018. A consensus report by the American Diabetes Association (ADA) and the European Association for the Study of Diabetes (EASD). Diabetologia 61, 2461–2498.

De Franco, E., Shaw-Smith, C., Flanagan, S.E., Edghill, E.L., Wolf, J., Otte, V., Ebinger, F., Varthakavi, P., Vasanthi, T., Edvardsson, S., et al. (2013). Biallelic PDX1 (insulin promoter factor 1) mutations causing neonatal diabetes without exocrine pancreatic insufficiency. Diabet. Med. 30, e197–e200.

Del Guerra, S., Lupi, R., Marselli, L., Masini, M., Bugliani, M., Sbrana, S., Torri, S., Pollera, M., Boggi, U., Mosca, F., et al. (2005). Functional and molecular defects of pancreatic islets in human type 2 diabetes. Diabetes 54, 727–735.

Deng, S., Vatamaniuk, M., Huang, X., Doliba, N., Lian, M.M., Frank, A., Velidedeoglu, E., Desai, N.M., Koeberlein, B., Wolf, B., et al. (2004). Structural and functional abnormalities in the islets isolated from type 2 diabetic subjects. Diabetes 53, 624–632.

Diedisheim, M., Oshima, M., Albagli, O., Huldt, C.W., Ahlstedt, I., Clausen, M., Menon, S., Aivazidis, A., Andreasson, A.C., Haynes, W.G., et al. (2018). Modeling human pancreatic beta cell dedifferentiation. Mol. Metab. 10, 74–86.

Donath, M.Y., Dalmas, É., Sauter, N.S., and Böni-Schnetzler, M. (2013). Inflammation in obesity and diabetes: islet dysfunction and therapeutic opportunity. Cell Metab. 17, 860–872.

Dotta, F., Censini, S., van Halteren, A.G., Marselli, L., Masini, M., Dionisi, S., Mosca, F., Boggi, U., Muda, A.O., Del Prato, S., et al. (2007). Coxsackie B4 virus infection of beta cells and natural killer cell insulitis in recent-onset type 1 diabetic patients. Proc. Natl. Acad. Sci. USA 104, 5115–5120.

Eguchi, K., and Nagai, R. (2017). Islet inflammation in type 2 diabetes and physiology. J. Clin. Invest. 127, 14–23.

Eizirik, D.L., Korbutt, G.S., and Hellerström, C. (1992). Prolonged exposure of human pancreatic islets to high glucose concentrations in vitro impairs the beta-cell function. J. Clin. Invest. 90, 1263–1268.

Eizirik, D.L., Pasquali, L., and Cnop, M. (2020). Pancreatic β-cells in type 1 and type 2 diabetes mellitus: different pathways to failure. Nat. Rev. Endocrinol. 16, 349–362.

Fadista, J., Vikman, P., Laakso, E.O., Mollet, I.G., Esguerra, J.L., Taneera, J., Storm, P., Osmark, P., Ladenvall, C., Prasad, R.B., et al. (2014). Global genomic and transcriptomic analysis of human pancreatic islets reveals novel genes influencing glucose metabolism. Proc. Natl. Acad. Sci. USA 111, 13924–13929.

Ferrannini, E. (2010). The stunned beta cell: a brief history. Cell Metab. 11, 349–352.

Fothergill-Gilmore, L.A., and Watson, H.C. (1989). The phosphoglycerate mutases. Adv. Enzymol. Relat. Areas Mol. Biol. 62, 227–313.

Frankish, A., Diekhans, M., Ferreira, A.M., Johnson, R., Jungreis, I., Loveland, J., Mudge, J.M., Sisu, C., Wright, J., Armstrong, J., et al. (2019). GENCODE reference annotation for the human and mouse genomes. Nucleic Acids Res. 47 (D1), D766–D773.

Fu, A., Eberhard, C.E., and Screaton, R.A. (2013). Role of AMPK in pancreatic beta cell function. Mol. Cell. Endocrinol. 366, 127–134.

Fuchsberger, C., Flannick, J., Teslovich, T.M., Mahajan, A., Agarwala, V., Gaulton, K.J., Ma, C., Fontanillas, P., Moutsianas, L., McCarthy, D.J., et al. (2016). The genetic architecture of type 2 diabetes. Nature 536, 41–47.

Furuta, H., Iwasaki, N., Oda, N., Hinokio, Y., Horikawa, Y., Yamagata, K., Yano, N., Sugahiro, J., Ogata, M., Ohgawara, H., et al. (1997). Organization and partial sequence of the hepatocyte nuclear factor-4 alpha/MODY1 gene and identification of a missense mutation, R127W, in a Japanese family with MODY. Diabetes 46, 1652–1657.

Galluzzi, L., Maiuri, M.C., Vitale, I., Zischka, H., Castedo, M., Zitvogel, L., and Kroemer, G. (2007). Cell death modalities: classification and pathophysiological implications. Cell Death Differ 14, 1237–1243.

Ganic, E., Singh, T., Luan, C., Fadista, J., Johansson, J.K., Cyphert, H.A., Bennet, H., Storm, P., Prost, G., Ahlenius, H., et al. (2016). MafA-Controlled Nicotinic Receptor Expression Is Essential for Insulin Secretion and Is Impaired in Patients with Type 2 Diabetes. Cell Rep. 14, 1991–2002.

Gargani, S., Thévenet, J., Yuan, J.E., Lefebvre, B., Delalleau, N., Gmyr, V., Hubert, T., Duhamel, A., Pattou, F., and Kerr-Conte, J. (2013). Adaptive changes of human islets to an obesogenic environment in the mouse. Diabetologia 56, 350–358.

Gill, R.M., Gabor, T.V., Couzens, A.L., and Scheid, M.P. (2013). The MYC-associated protein CDCA7 is phosphorylated by AKT to regulate MYC-dependent apoptosis and transformation. Mol. Cell. Biol. 33, 498–513.

Giusti, L., Molinaro, A., Alessandrì, M.G., Boldrini, C., Ciregia, F., Lacerenza, S., Ronci, M., Urbani, A., Cioni, G., Mazzoni, M.R., et al. (2019). Brain mitochondrial proteome alteration driven by creatine deficiency suggests novel therapeutic venues for creatine deficiency syndromes. Neuroscience 409, 276–289.

Grarup, N., Overvad, M., Sparsø, T., Witte, D.R., Pisinger, C., Jørgensen, T., Yamauchi, T., Hara, K., Maeda, S., Kadowaki, T., et al. (2011). The diabetogenic VPS13C/C2CD4A/C2CD4B rs7172432 variant impairs glucose-stimulated insulin response in 5,722 non-diabetic Danish individuals. Diabetologia 54, 789–794.

Gunton, J.E., Kulkarni, R.N., Yim, S., Okada, T., Hawthorne, W.J., Tseng, Y.H., Roberson, R.S., Ricordi, C., O'Connell, P.J., Gonzalez, F.J., and Kahn, C.R. (2005). Loss of ARNT/HIF1beta mediates altered gene expression and pancreatic-islet dysfunction in human type 2 diabetes. Cell 122, 337–349.

Halban, P.A., Polonsky, K.S., Bowden, D.W., Hawkins, M.A., Ling, C., Mather, K.J., Powers, A.C., Rhodes, C.J., Sussel, L., and Weir, G.C. (2014). β-Cell failure in type 2 diabetes: postulated mechanisms and prospects for prevention and treatment. Diabetes Care 37, 1751–1758.

Hall, E., Volkov, P., Dayeh, T., Bacos, K., Rönn, T., Nitert, M.D., and Ling, C. (2014). Effects of palmitate on genome-wide mRNA expression and DNA methylation patterns in human pancreatic islets. BMC Med. 12, 103.

Hall, E., Jönsson, J., Ofori, J.K., Volkov, P., Perfilyev, A., Dekker Nitert, M., Eliasson, L., Ling, C., and Bacos, K. (2019). Glucolipotoxicity Alters Insulin Secretion via Epigenetic Changes in Human Islets. Diabetes 68, 1965–1974.

Harder, M.N., Appel, E.V., Grarup, N., Gjesing, A.P., Ahluwalia, T.S., Jørgensen, T., Christensen, C., Brandslund, I., Linneberg, A., Sørensen, T.I., et al. (2015). The type 2 diabetes risk allele of TMEM154-rs6813195 associates with decreased beta cell function in a study of 6,486 Danes. PLOS ONE 10, e0120890.

Hart, N.J., and Powers, A.C. (2019). Use of human islets to understand islet biology and diabetes: progress, challenges and suggestions. Diabetologia 62, 212–222.

Hitosugi, T., Zhou, L., Elf, S., Fan, J., Kang, H.B., Seo, J.H., Shan, C., Dai, Q., Zhang, L., Xie, J., et al. (2012). Phosphoglycerate mutase 1 coordinates glycolysis and biosynthesis to promote tumor growth. Cancer Cell 22, 585–600.

Hodson, D.J., Mitchell, R.K., Marselli, L., Pullen, T.J., Gimeno Brias, S., Semplici, F., Everett, K.L., Cooper, D.M., Bugliani, M., Marchetti, P., et al. (2014). ADCY5 couples glucose to insulin secretion in human islets. Diabetes 63, 3009–3021.

Isserlin, R., Merico, D., Alikhani-Koupaei, R., Gramolini, A., Bader, G.D., and Emili, A. (2010). Pathway analysis of dilated cardiomyopathy using global proteomic profiling and enrichment maps. Proteomics 10, 1316–1327.

Janikiewicz, J., Hanzelka, K., Kozinski, K., Kolczynska, K., and Dobrzyn, A. (2015). Islet β-cell failure in type 2 diabetes–within the network of toxic lipids. Biochem. Biophys. Res. Commun. 460, 491–496.

Kahn, S.E. (2003). The relative contributions of insulin resistance and beta-cell dysfunction to the pathophysiology of type 2 diabetes. Diabetologia 46, 3–19.

Kashyap, S., Belfort, R., Gastaldelli, A., Pratipanawatr, T., Berria, R., Pratipanawatr, W., Bajaj, M., Mandarino, L., DeFronzo, R., and Cusi, K. (2003). A sustained increase in plasma free fatty acids impairs insulin secretion in nondiabetic subjects genetically predisposed to develop type 2 diabetes. Diabetes 52, 2461–2474.

Khamis, A., Canouil, M., Siddiq, A., Crouch, H., Falchi, M., Bulow, M.V., Ehehalt, F., Marselli, L., Distler, M., Richter, D., et al. (2019). Laser capture

microdissection of human pancreatic islets reveals novel eQTLs associated with type 2 diabetes. Mol. Metab. *24*, 98–107.

Kim, D., Pertea, G., Trapnell, C., Pimentel, H., Kelley, R., and Salzberg, S.L. (2013). TopHat2: accurate alignment of transcriptomes in the presence of insertions, deletions and gene fusions. Genome Biol. *14*, R36.

Kosaka, K., Kuzuya, T., Akanuma, Y., and Hagura, R. (1980). Increase in insulin response after treatment of overt maturity-onset diabetes is independent of the mode of treatment. Diabetologia *18*, 23–28.

Kramer, C.K., Zinman, B., and Retnakaran, R. (2013). Short-term intensive insulin therapy in type 2 diabetes mellitus: a systematic review and meta-analysis. Lancet Diabetes Endocrinol. *1*, 28–34.

Kycia, I., Wolford, B.N., Huyghe, J.R., Fuchsberger, C., Vadlamudi, S., Kursawe, R., Welch, R.P., Albanus, R.D., Uyar, A., Khetan, S., et al. (2018). A Common Type 2 Diabetes Risk Variant Potentiates Activity of an Evolutionarily Conserved Islet Stretch Enhancer and Increases C2CD4A and C2CD4B Expression. Am. J. Hum. Genet. *102*, 620–635.

Lascar, N., Brown, J., Pattison, H., Barnett, A.H., Bailey, C.J., and Bellary, S. (2018). Type 2 diabetes in adolescents and young adults. Lancet Diabetes Endocrinol. *6*, 69–80.

Lean, M.E., Leslie, W.S., Barnes, A.C., Brosnahan, N., Thom, G., McCombie, L., Peters, C., Zhyzhneuskaya, S., Al-Mrabeh, A., Hollingsworth, K.G., et al. (2018). Primary care-led weight management for remission of type 2 diabetes (DiRECT): an open-label, cluster-randomised trial. Lancet *391*, 541–551.

Lemaire, K., Granvik, M., Schraenen, A., Goyvaerts, L., Van Lommel, L., Gómez-Ruiz, A., In 't Veld, P., Gilon, P., and Schuit, F. (2017). How stable is repression of disallowed genes in pancreatic islets in response to metabolic stress? PLOS ONE *12*, e0181651.

Li, L.O., Mashek, D.G., An, J., Doughman, S.D., Newgard, C.B., and Coleman, R.A. (2006). Overexpression of rat long chain acyl-coa synthetase 1 alters fatty acid metabolism in rat primary hepatocytes. J. Biol. Chem. *281*, 37246–37255.

Linxweiler, M., Schick, B., and Zimmermann, R. (2017). Let's talk about Secs: Sec61, Sec62 and Sec63 in signal transduction, oncology and personalized medicine. Signal Transduct. Target. Ther. *2*, 17002.

Love, M.I., Huber, W., and Anders, S. (2014). Moderated estimation of fold change and dispersion for RNA-seq data with DESeq2. Genome Biol. *15*, 550.

Lu, Z., Zhou, L., Killela, P., Rasheed, A.B., Di, C., Poe, W.E., McLendon, R.E., Bigner, D.D., Nicchitta, C., and Yan, H. (2009). Glioblastoma proto-oncogene SEC61gamma is required for tumor cell survival and response to endoplasmic reticulum stress. Cancer Res. *69*, 9105–9111.

Ludvik, A.E., Pusec, C.M., Priyadarshini, M., Angueira, A.R., Guo, C., Lo, A., Hershenhouse, K.S., Yang, G.Y., Ding, X., Reddy, T.E., et al. (2016). HKDC1 Is a Novel Hexokinase Involved in Whole-Body Glucose Use. Endocrinology *157*, 3452–3461.

Lupi, R., Dotta, F., Marselli, L., Del Guerra, S., Masini, M., Santangelo, C., Patané, G., Boggi, U., Piro, S., Anello, M., et al. (2002). Prolonged exposure to free fatty acids has cytostatic and pro-apoptotic effects on human pancreatic islets: evidence that beta-cell death is caspase mediated, partially dependent on ceramide pathway, and Bcl-2 regulated. Diabetes *51*, 1437–1442.

Lytrivi, M., Igoillo-Esteve, M., and Cnop, M. (2018). Inflammatory stress in islet β-cells: therapeutic implications for type 2 diabetes? Curr. Opin. Pharmacol. *43*, 40–45.

Lytrivi, M., Castell, A.L., Poitout, V., and Cnop, M. (2020). Recent Insights Into Mechanisms of β-Cell Lipo- and Glucolipotoxicity in Type 2 Diabetes. J. Mol. Biol. *432*, 1514–1534.

Mahajan, A., Taliun, D., Thurner, M., Robertson, N.R., Torres, J.M., Rayner, N.W., Payne, A.J., Steinthorsdottir, V., Scott, R.A., Grarup, N., et al. (2018). Fine-mapping type 2 diabetes loci to single-variant resolution using high-density imputation and islet-specific epigenome maps. Nat. Genet. *50*, 1505–1513.

Marchetti, P. (2016). Islet inflammation in type 2 diabetes. Diabetologia *59*, 668–672.

Marchetti, P., Bugliani, M., Lupi, R., Marselli, L., Masini, M., Boggi, U., Filipponi, F., Weir, G.C., Eizirik, D.L., and Cnop, M. (2007). The endoplasmic re-

ticulum in pancreatic beta cells of type 2 diabetes patients. Diabetologia *50*, 2486–2494.

Marchetti, P., Lupi, R., Del Guerra, S., Bugliani, M., D'Aleo, V., Occhipinti, M., Boggi, U., Marselli, L., and Masini, M. (2009). Goals of treatment for type 2 diabetes: beta-cell preservation for glycemic control. Diabetes Care *32* (*Suppl 2*), S178–S183.

Marchetti, P., Bugliani, M., De Tata, V., Suleiman, M., and Marselli, L. (2017). Pancreatic beta cell identity in humans and the role of type 2 diabetes. Front. Cell Dev. Biol. *5*, 55.

Marchetti, P., Schulte, A.M., Marselli, L., Schoniger, E., Bugliani, M., Kramer, W., Overbergh, L., Ullrich, S., Gloyn, A.L., Ibberson, M., et al. (2019). Fostering improved human islet research: a European perspective. Diabetologia *62*, 1514–1516.

Marchetti, P., Suleiman, M., De Luca, C., Baronti, W., Bosi, E., Tesi, M., and Marselli, L. (2020). A direct look at the dysfunction and pathology of the β cells in human type 2 diabetes. Semin. Cell Dev. Biol. *103*, 83–93.

Maridas, D.E., DeMambro, V.E., Le, P.T., Mohan, S., and Rosen, C.J. (2017). IGFBP4 Is Required for Adipogenesis and Influences the Distribution of Adipose Depots. Endocrinology *158*, 3488–3500.

Marselli, L., Thorne, J., Dahiya, S., Sgroi, D.C., Sharma, A., Bonner-Weir, S., Marchetti, P., and Weir, G.C. (2010). Gene expression profiles of Beta-cell enriched tissue obtained by laser capture microdissection from subjects with type 2 diabetes. PLOS ONE *5*, e11499.

Marselli, L., Bugliani, M., Suleiman, M., Olimpico, F., Masini, M., Petrini, M., Boggi, U., Filipponi, F., Syed, F., and Marchetti, P. (2013). β-Cell inflammation in human type 2 diabetes and the role of autophagy. Diabetes Obes. Metab. *15* (*Suppl 3*), 130–136.

Marselli, L., Suleiman, M., Masini, M., Campani, D., Bugliani, M., Syed, F., Martino, L., Focosi, D., Scatena, F., Olimpico, F., et al. (2014). Are we overestimating the loss of beta cells in type 2 diabetes? Diabetologia *57*, 362–365.

Marshak, S., Leibowitz, G., Bertuzzi, F., Socci, C., Kaiser, N., Gross, D.J., Cerasi, E., and Melloul, D. (1999). Impaired beta-cell functions induced by chronic exposure of cultured human pancreatic islets to high glucose. Diabetes *48*, 1230–1236.

Martinez-Sanchez, A., Nguyen-Tu, M.S., Leclerc, I., and Rutter, G.A. (2018). Manipulation and Measurement of AMPK Activity in Pancreatic Islets. Methods Mol. Biol. *1732*, 413–431.

Masini, M., Bugliani, M., Lupi, R., del Guerra, S., Boggi, U., Filipponi, F., Marselli, L., Masiello, P., and Marchetti, P. (2009). Autophagy in human type 2 diabetes pancreatic beta cells. Diabetologia *52*, 1083–1086.

McCarthy, D.J., Chen, Y., and Smyth, G. (2012). Differential expression analysis of multifactor RNA-Seq experiments with respect to biological variation. Nucleic Acids Res *40*, 4288–4297.

McMahon, S.B. (2014). MYC and the control of apoptosis. Cold Spring Harb. Perspect. Med. *4*, a014407.

Merico, D., Isserlin, R., Stueker, O., Emili, A., and Bader, G.D. (2010). Enrichment map: a network-based method for gene-set enrichment visualization and interpretation. PLOS ONE *5*, e13984.

Miguel-Escalada, I., Bonàs-Guarch, S., Cebola, I., Ponsa-Cobas, J., Mendieta-Esteban, J., Atla, G., Javierre, B.M., Rolando, D.M.Y., Farabella, I., Morgan, C.C., et al. (2019). Human pancreatic islet three-dimensional chromatin architecture provides insights into the genetics of type 2 diabetes. Nat. Genet. *51*, 1137–1148.

Mingrone, G., Panunzi, S., De Gaetano, A., Guidone, C., Iaconelli, A., Nanni, G., Castagneto, M., Bornstein, S., and Rubino, F. (2015). Bariatric-metabolic surgery versus conventional medical treatment in obese patients with type 2 diabetes: 5 year follow-up of an open-label, single-centre, randomised controlled trial. Lancet *386*, 964–973.

Miyazaki, J., Araki, K., Yamato, E., Ikegami, H., Asano, T., Shibasaki, Y., Oka, Y., and Yamamura, K. (1990). Establishment of a pancreatic beta cell line that retains glucose-inducible insulin secretion: special reference to expression of glucose transporter isoforms. Endocrinology *127*, 126–132.

Montgomery, S.B., Sammeth, M., Gutierrez-Arcelus, M., Lach, R.P., Ingle, C., Nisbett, J., Guigo, R., and Dermitzakis, E.T. (2010). Transcriptome genetics using second generation sequencing in a Caucasian population. Nature *464*, 773–777.

Moore, F., Cunha, D.A., Mulder, H., and Eizirik, D.L. (2012). Use of RNA interference to investigate cytokine signal transduction in pancreatic beta cells. Methods Mol. Biol. *820*, 179–194.

Nica, A.C., Ongen, H., Irminger, J.C., Bosco, D., Berney, T., Antonarakis, S.E., Halban, P.A., and Dermitzakis, E.T. (2013). Cell-type, allelic, and genetic signatures in the human pancreatic beta cell transcriptome. Genome Res. *23*, 1554–1562.

Nirmal, A.J., Regan, T., Shih, B.B., Hume, D.A., Sims, A.H., and Freeman, T.C. (2018). Immune Cell Gene Signatures for Profiling the Microenvironment of Solid Tumors. Cancer Immunol. Res. *6*, 1388–1400.

Okuda, J., Niizuma, S., Shioi, T., Kato, T., Inuzuka, Y., Kawashima, T., Tamaki, Y., Kawamoto, A., Tanada, Y., Iwanaga, Y., et al. (2013). Persistent overexpression of phosphoglycerate mutase, a glycolytic enzyme, modifies energy metabolism and reduces stress resistance of heart in mice. PLOS ONE *8*, e72173.

Olbrot, M., Rud, J., Moss, L.G., and Sharma, A. (2002). Identification of beta-cell-specific insulin gene transcription factor RIPE3b1 as mammalian MafA. Proc. Natl. Acad. Sci. USA *99*, 6737–6742.

Oliveira, A.F., Cunha, D.A., Ladriere, L., Igoillo-Esteve, M., Bugliani, M., Marchetti, P., and Cnop, M. (2015). In vitro use of free fatty acids bound to albumin: a comparison of protocols. Biotechniques *58*, 228–233.

Osipovich, A.B., Long, Q., Manduchi, E., Gangula, R., Hipkens, S.B., Schneider, J., Okubo, T., Stoeckert, C.J., Jr., Takada, S., and Magnuson, M.A. (2014). Insm1 promotes endocrine cell differentiation by modulating the expression of a network of genes that includes Neurog3 and Ripply3. Development *141*, 2939–2949.

Ottosson-Laakso, E., Krus, U., Storm, P., Prasad, R.B., Oskolkov, N., Ahlqvist, E., Fadista, J., Hansson, O., Groop, L., and Vikman, P. (2017). Glucose-Induced Changes in Gene Expression in Human Pancreatic Islets: Causes or Consequences of Chronic Hyperglycemia. Diabetes *66*, 3013–3028.

Paolisso, G., Gambardella, A., Amato, L., Tortoriello, R., D'Amore, A., Varricchio, M., and D'Onofrio, F. (1995). Opposite effects of short- and long-term fatty acid infusion on insulin secretion in healthy subjects. Diabetologia *38*, 1295–1299.

Patro, R., Duggal, G., Love, M.I., Irizarry, R.A., and Kingsford, C. (2017). Salmon provides fast and bias-aware quantification of transcript expression. Nat. Methods *14*, 417–419.

Pieragostino, D., Lanuti, P., Cicalini, I., Cufaro, M.C., Ciccocioppo, F., Ronci, M., Simeone, P., Onofrj, M., van der Pol, E., Fontana, A., et al. (2019). Proteomics characterization of extracellular vesicles sorted by flow cytometry reveals a disease-specific molecular cross-talk from cerebrospinal fluid and tears in multiple sclerosis. J. Proteomics *204*, 103403.

Plaisier, S.B., Taschereau, R., Wong, J.A., and Graeber, T.G. (2010). Rank-rank hypergeometric overlap: identification of statistically significant overlap between gene-expression signatures. Nucleic Acids Res. *38*, e169.

Poitout, V., and Robertson, R.P. (2008). Glucolipotoxicity: fuel excess and beta-cell dysfunction. Endocr. Rev. *29*, 351–366.

Poitout, V., Amyot, J., Semache, M., Zarrouki, B., Hagman, D., and Fontés, G. (2010). Glucolipotoxicity of the pancreatic beta cell. Biochim. Biophys. Acta *1801*, 289–298.

Poitout, V., Satin, L.S., Kahn, S.E., Stoffers, D.A., Marchetti, P., Gannon, M., Verchere, C.B., Herold, K.C., Myers, M.G., Jr., and Marshall, S.M. (2019). A Call for Improved Reporting of Human Islet Characteristics in Research Articles. Diabetes *68*, 239–240.

Pullen, T.J., Khan, A.M., Barton, G., Butcher, S.A., Sun, G., and Rutter, G.A. (2010). Identification of genes selectively disallowed in the pancreatic islet. Islets *2*, 89–95.

Pullen, T.J., Huising, M.O., and Rutter, G.A. (2017). Analysis of Purified Pancreatic Islet Beta and Alpha Cell Transcriptomes Reveals 11β-Hydroxysteroid Dehydrogenase (Hsd11b1) as a Novel Disallowed Gene. Front. Genet. *8*, 41.

Raudvere, U., Kolberg, L., Kuzmin, I., Arak, T., Adler, P., Peterson, H., and Vilo, J. (2019). g:Profiler: a web server for functional enrichment analysis and conversions of gene lists (2019 update). Nucleic Acids Res. *47 (W1)*, W191–W198.

Ravassard, P., Hazhouz, Y., Pechberty, S., Bricout-Neveu, E., Armanet, M., Czernichow, P., and Scharfmann, R. (2011). A genetically engineered human pancreatic β cell line exhibiting glucose-inducible insulin secretion. J. Clin. Invest. *121*, 3589–3597.

Robertson, R.P. (2009). Beta-cell deterioration during diabetes: what's in the gun? Trends Endocrinol. Metab. *20*, 388–393.

Robertson, R.P., Harmon, J., Tran, P.O., and Poitout, V. (2004). Beta-cell glucose toxicity, lipotoxicity, and chronic oxidative stress in type 2 diabetes. Diabetes *53 (Suppl 1)*, S119–S124.

Robinson, M.D., McCarthy, D.J., and Smyth, G.K. (2010). edgeR: a Bioconductor package for differential expression analysis of digital gene expression data. Bioinformatics *26*, 139–140.

Ronci, M., Leporini, L., Felaco, P., Sirolli, V., Pieroni, L., Greco, V., Aceto, A., Urbani, A., and Bonomini, M. (2018). Proteomic Characterization of a New asymmetric Cellulose Triacetate Membrane for Hemodialysis. Proteomics Clin. Appl. *12*, e1700140.

Russell, R., Carnese, P.P., Hennings, T.G., Walker, E.M., Russ, H.A., Liu, J.S., Giacometti, S., Stein, R., and Hebrok, M. (2020). Loss of the transcription factor MAFB limits β-cell derivation from human PSCs. Nat. Commun. *11*, 2742.

Rutter, G.A., Pullen, T.J., Hodson, D.J., and Martinez-Sanchez, A. (2015). Pancreatic β-cell identity, glucose sensing and the control of insulin secretion. Biochem. J. *466*, 203–218.

Shimoda, Y., Matsuo, K., Kitamura, Y., Ono, K., Ueyama, T., Matoba, S., Yamada, H., Wu, T., Chen, J., Emoto, N., and Ikeda, K. (2015). Diabetes-Related Ankyrin Repeat Protein (DARP/Ankrd23) Modifies Glucose Homeostasis by Modulating AMPK Activity in Skeletal Muscle. PLOS ONE *10*, e0138624.

Shuldiner, A.R., and McLenithan, J.C. (2004). Genes and pathophysiology of type 2 diabetes: more than just the Randle cycle all over again. J. Clin. Invest. *114*, 1414–1417.

Six, E., Lagresle-Peyrou, C., Susini, S., De Chappedelaine, C., Sigrist, N., Sadek, H., Chouteau, M., Cagnard, N., Fontenay, M., Hermine, O., et al. (2015). AK2 deficiency compromises the mitochondrial energy metabolism required for differentiation of human neutrophil and lymphoid lineages. Cell Death Dis. *6*, e1856.

Sjöström, L., Lindroos, A.K., Peltonen, M., Torgerson, J., Bouchard, C., Carlsson, B., Dahlgren, S., Larsson, B., Narbro, K., Sjöström, C.D., et al.; Swedish Obese Subjects Study Scientific Group (2004). Lifestyle, diabetes, and cardiovascular risk factors 10 years after bariatric surgery. N. Engl. J. Med. *351*, 2683–2693.

Solimena, M., Schulte, A.M., Marselli, L., Ehehalt, F., Richter, D., Kleeberg, M., Mziaut, H., Knoch, K.P., Parnis, J., Bugliani, M., et al. (2018). Systems biology of the IMIDIA biobank from organ donors and pancreatectomised patients defines a novel transcriptomic signature of islets from individuals with type 2 diabetes. Diabetologia *61*, 641–657.

Solomon, T.P., Knudsen, S.H., Karstoft, K., Winding, K., Holst, J.J., and Pedersen, B.K. (2012). Examining the effects of hyperglycemia on pancreatic endocrine function in humans: evidence for in vivo glucotoxicity. J. Clin. Endocrinol. Metab. *97*, 4682–4691.

Steven, S., Hollingsworth, K.G., Al-Mrabeh, A., Avery, L., Aribisala, B., Caslake, M., and Taylor, R. (2016). Very Low-Calorie Diet and 6 Months of Weight Stability in Type 2 Diabetes: Pathophysiological Changes in Responders and Nonresponders. Diabetes Care *39*, 808–815.

Støy, J., Edghill, E.L., Flanagan, S.E., Ye, H., Paz, V.P., Pluzhnikov, A., Below, J.E., Hayes, M.G., Cox, N.J., Lipkind, G.M., et al.; Neonatal Diabetes International Collaborative Group (2007). Insulin gene mutations as a cause of permanent neonatal diabetes. Proc. Natl. Acad. Sci. USA *104*, 15040–15044.

Subramanian, A., Tamayo, P., Mootha, V.K., Mukherjee, S., Ebert, B.L., Gillette, M.A., Paulovich, A., Pomeroy, S.L., Golub, T.R., Lander, E.S., and Mesirov, J.P. (2005). Gene set enrichment analysis: a knowledge-based approach for interpreting genome-wide expression profiles. Proc. Natl. Acad. Sci. USA *102*, 15545–15550.

Sun, Q., Song, K., Shen, X., and Cai, Y. (2012). The association between KCNQ1 gene polymorphism and type 2 diabetes risk: a meta-analysis. PLOS ONE *7*, e48578.

Sun, G., da Silva Xavier, G., Gorman, T., Priest, C., Solomou, A., Hodson, D.J., Foretz, M., Viollet, B., Herrera, P.L., Parker, H., et al. (2015). LKB1 and AMPKα1 are required in pancreatic alpha cells for the normal regulation of glucagon secretion and responses to hypoglycemia. Mol. Metab. *4*, 277–286.

Swisa, A., Avrahami, D., Eden, N., Zhang, J., Feleke, E., Dahan, T., Cohen-Tayar, Y., Stolovich-Rain, M., Kaestner, K.H., Glaser, B., et al. (2017a). PAX6 maintains β cell identity by repressing genes of alternative islet cell types. J. Clin. Invest. *127*, 230–243.

Swisa, A., Glaser, B., and Dor, Y. (2017b). Metabolic Stress and Compromised Identity of Pancreatic Beta Cells. Front. Genet. *8*, 21.

Taneera, J., Lang, S., Sharma, A., Fadista, J., Zhou, Y., Ahlqvist, E., Jonsson, A., Lyssenko, V., Vikman, P., Hansson, O., et al. (2012). A systems genetics approach identifies genes and pathways for type 2 diabetes in human islets. Cell Metab. *16*, 122–134.

Taylor, R., Al-Mrabeh, A., Zhyzhneuskaya, S., Peters, C., Barnes, A.C., Aribisala, B.S., Hollingsworth, K.G., Mathers, J.C., Sattar, N., and Lean, M.E.J. (2018). Remission of Human Type 2 Diabetes Requires Decrease in Liver and Pancreas Fat Content but Is Dependent upon Capacity for β Cell Recovery. Cell Metab. *28*, 547–556.e3.

Taylor, R., Al-Mrabeh, A., and Sattar, N. (2019). Understanding the mechanisms of reversal of type 2 diabetes. Lancet Diabetes Endocrinol. *7*, 726–736.

Thorrez, L., Laudadio, I., Van Deun, K., Quintens, R., Hendrickx, N., Granvik, M., Lemaire, K., Schraenen, A., Van Lommel, L., Lehnert, S., et al. (2011). Tissue-specific disallowance of housekeeping genes: the other face of cell differentiation. Genome Res. *21*, 95–105.

Touati, A., Errea-Dorronsoro, J., Nouri, S., Halleb, Y., Pereda, A., Mahdhaoui, N., Ghith, A., Saad, A., Perez de Nanclares, G., and H'mida Ben Brahim, D. (2019). Transient neonatal diabetes mellitus and hypomethylation at additional imprinted loci: novel ZFP57 mutation and review on the literature. Acta Diabetol. *56*, 301–307.

UK Prospective Diabetes Study (UKPDS) Group (1998). Intensive blood-glucose control with sulphonylureas or insulin compared with conventional treatment and risk of complications in patients with type 2 diabetes (UKPDS 33). Lancet *352*, 837–853.

van de Bunt, M., Cortes, A., Brown, M.A., Morris, A.P., and McCarthy, M.I.; IGAS Consortium (2015). Evaluating the performance of fine-mapping strategies at common variant GWAS loci. PLOS Genet. *11*, e1005535.

Varshney, A., Scott, L.J., Welch, R.P., Erdos, M.R., Chines, P.S., Narisu, N., Albanus, R.D., Orchard, P., Wolford, B.N., Kursawe, R., et al.; NISC Comparative Sequencing Program (2017). Genetic regulatory signatures underlying islet gene expression and type 2 diabetes. Proc. Natl. Acad. Sci. USA *114*, 2301–2306.

Viñuela, A., Varshney, A., van de Bunt, M., Prasad, R.B., Asplund, O., Bennett, A., Boehnke, M., Brown, A.A., Erdos, M.R., Fadista, J., et al. (2020). Genetic variant effects on gene expression in human pancreatic islets and their implications for T2D. Nat. Commun. *11*, 4912.

Wang, Y.J., and Kaestner, K.H. (2019). Single-cell RNA-seq of the pancreatic islets–a promise not yet fulfilled? Cell Metab. *29*, 539–544.

Weir, G.C., Marselli, L., Marchetti, P., Katsuta, H., Jung, M.H., and Bonner-Weir, S. (2009). Towards better understanding of the contributions of overwork and glucotoxicity to the beta-cell inadequacy of type 2 diabetes. Diabetes Obes. Metab. *11* (*Suppl 4*), 82–90.

White, M.G., Shaw, J.A., and Taylor, R. (2016). Type 2 diabetes: the pathologic basis of reversible β-cell dysfunction. Diabetes Care *39*, 2080–2088.

Wiederkehr, A., and Wollheim, C.B. (2009). Linking fatty acid stress to beta-cell mitochondrial dynamics. Diabetes *58*, 2185–2186.

Yang, J.-K., Lu, J., Yuan, S.-S., Asan, Cao, X., Qiu, H.-Y., Shi, T.-T., Yang, F.-Y., Li, Q., Liu, C.-P., et al. (2018). From hyper- to hypoinsulinemia and diabetes: effect of KCNH6 on insulin secretion. Cell Rep. *25*, 3800–3810.

STAR★METHODS

KEY RESOURCES TABLE

REAGENT or RESOURCE	SOURCE	IDENTIFIER
Antibodies		
Guinea pig polyclonal anti-insulin	Invitrogen	Cat# 18-0067; RRID: AB_86637
Rabbit polyclonal anti-glucagon	Dako	Cat# A0565; RRID: AB_10013726
Mouse monoclonal anti-chromogranin A (clone LK2H10)	Ventana	Cat# 760-2519; RRID: AB_2335955
anti-pAMPK	Abcam	2535S; RRID:AB_331250
pRaptor	Abcam	2083S; RRID:AB_2249475
pACC	Abcam	3661S; RRID:AB_330337
AMPK	Abcam	2532S; RRID:AB_330331
Raptor	Abcam	2280S; RRID:AB_561245
ACC	Abcam	3662S; RRID:AB_2219400
Rabbit polyclonal anti-ANKRD23	Abcam	Cat# ab118210; RRID: AB_10899509
Mouse monoclonal anti-α-tubulin (clone B-5-1-2)	Sigma-Aldrich	Cat# T5168; RRID: AB_477579
Goat polyclonal anti-rabbit IgG H&L (HRP)	Abcam	Cat# ab6721; RRID: AB_955447
Rabbit polyclonal cleaved caspase-3 (Asp175) antibody	Cell Signaling	Cat# 9661; RRID: AB_2341188
Rat polyclonal cleaved caspase-9 (Asp353) antibody	Cell Signaling	Cat #9507; RRID: AB_2228625
Mouse monoclonal anti-α-tubulin (clone DM1A)	Sigma-Aldrich	Cat# T9026; RRID: AB_477593)
Goat Anti-Rabbit IgG - H&L Polyclonal antibody, Hrp Conjugated	Abcam	Cat# ab6721; RRID:AB_955447
Bacterial and Virus Strains		
Adenovirus expressing GFP	Imperial College London (Home-made)	N/A
Adenovirus expressing mouse Ankrd23	Vector Biolabs	ADV-252662
Biological Samples		
Human pancreatic islets	University of Pisa, Pisa	N/A
Chemicals, Peptides, and Recombinant Proteins		
D-Glucose	Sigma	Cat# G7528
Sodium palmitate	Sigma	Cat# P9767
Sodium oleate	Sigma	Cat# O7501
Bovine serum albumin fraction V, fatty acid free	Sigma	Cat# 10775835001
Critical Commercial Assays		
Histostain-Plus kits	Invitrogen	Cat# 85-9643
DIAsource INS-IRMA	DIAsource ImmunoAssays S.A.	Cat# KIP1251
Deposited Data		
Genome Reference Consortium Human Build 37 (GRCh37/hg19)	Genome Reference Consortium	https://www.ncbi.nlm.nih.gov/grc/human
Genecode release 18	The GENCODE project	https://www.gencodegenes.org
Genome Reference Consortium Human Build 38 (GRCh38)	Genome Reference Consortium	https://www.ncbi.nlm.nih.gov/grc/human
Human islet RNA-seq	This paper	https://www.ncbi.nlm.nih.gov/geo/ GSE159984
NeXtprot database	Swiss Institute of Bioinformatics	https://www.nextprot.org/

(Continued on next page)

Continued

REAGENT or RESOURCE	SOURCE	IDENTIFIER
Experimental Models: Cell Lines		
Human EndoC-βH1 cell line	R. Scharfmann, Cochin Institute, Paris, France	N/A
Rat INS-1E cell line	C Wollheim, University of Geneva Medical Centre, Switzerland	RRID:CVCL_0351
Mouse MIN6B1 cell line	Philippe Halban, University of Geneva Medical Centre, Switzerland	N/A
Oligonucleotides		
Allstars Negative Control siRNA	QIAGEN	Cat# 1027280
Rat Sec61G siRNA predesigned, silencer select: 5′-AGCUCAUGAAGUAAAAGUUtt −3′	Invitrogen	Cat# s184396
ON-TARGETplus Rat Sec61 g (689134) siRNA – SMARTpool: 5′- GGUGACAAGCUCAUGAAGU −3′ 5′- CCUGGAUGCUUUGUGGUUU-3′ 5′- UGUGGGUGGCUGAGUCUUU-3′ 5′- UCAUCGUGGGACUGGUGAA-3′	Dharmacon	L-110743-00-0005
Custom designed stealth siRNA human SEC61G: 5′-GCCAAGUCGGCAGUUUG UAAAGGA −3′	Invitrogen	Cat# 10620319
Software and Algorithms		
Leica MetaMorph® software, v1.8.0	Leica	N/A
GraphPad Prism v8.4.2	GraphPad Software, San Diego, CA, USA	https://www.graphpad.com
TopHat 2 v2.0.13	Center for Computational Biology at Johns Hopkins University	http://ccb.jhu.edu/software/tophat/index.shtml
Flux Capacitor v. 1.2.4	Montgomery et al., 2010	http://confluence.sammeth.net
R/Bioconductor package EdgeR v3.30.1	McCarthy et al., 2012	http://bioconductor.org
Salmon v13.2	Patro et al., 2017	https://combine-lab.github.io/salmon/
R DESeq2 package v1.24.0	Love et al., 2014	http://www.bioconductor.org/packages/release/bioc/html/DESeq2.html
Rank-Rank Hypergeometric Overlap v1.28.0	University of California, Los Angeles	https://systems.crump.ucla.edu/rankrank/;
R package gprofiler2 v0.1.9	ELIXIR infrastructure	https://biit.cs.ut.ee/gprofiler/page/r
Gene Set Enrichment Analysis (GSEA) v3.0	University of California San Diego and Broad Institute	https://www.gsea-msigdb.org/gsea/index.jsp
Enrichment Map v3.1	University of Toronto	http://baderlab.org/Software/EnrichmentMap/
Cytoscape v3.6	National Resource for Network Biology	https://cytoscape.org/
PEAKS Studio v7.5	Bioinformatic Solutions Inc, Waterloo, Canada	https://www.bioinfor.com/peaks-studio/
Other		
Leica DM5500 B microscope	Leica	N/A
DFC310 FX camera	Leica	N/A

RESOURCE AVAILABILITY

Lead Contact
Further information and requests for resources and reagents should be directed to and will be fulfilled by the Lead Contact, Piero Marchetti (piero.marchetti@med.unipi.it).

Materials Availability
This study did not generate new unique reagents.

Data and Code Availability
RNA sequencing data have been submitted to the NCBI Gene Expression Omnibus (GEO; https://www.ncbi.nlm.nih.gov/geo/). The accession number for expression data reported in this paper is GSE159984. Original data are available from the lead contact upon reasonable request.

EXPERIMENTAL MODEL AND SUBJECT DETAILS

Human pancreatic islets
Islets were prepared from the pancreas of 26 ND organ donors (16 females, 10 males, age: 72 ± 3 years, BMI: 24.6 ± 0.7 Kg/m^2) (Marselli et al., 2014; Marchetti et al., 2007). The main clinical characteristics of each donor are provided in Table S1, together with features of the processed pancreases and isolated islets. The islets were studied in terms of function, morphology and transcriptome evaluation. In a separate set of experiments, islets were obtained from the pancreas of 28 T2D (9 females and 19 males, age: 73.6 ± 1.5 years, BMI: 26.3 ± 0.7 Kg/m^2) and 58 ND (30 females and 28 males, age: 64.4 ± 2.1 years, BMI: 25.3 ± 0.5 Kg/m^2) donors (detailed information on these donors is also provided in Table S1, according to Hart and Powers, 2019). The transcriptome of these two islet groups was analyzed by RNaseq and compared. Part of these preparations (43 ND and 15 T2D) have been previously used to assess islet gene expression features by microarray analysis (Solimena et al., 2018). Pancreas and islet handling were conducted with permission by the Ethics Committee of the University of Pisa, upon written consent of donors' next-of-kin.

Cell lines
For validation studies, three different beta cell lines were used. The EndoC-βH1 cell line was cultured in DMEM cointaining 5.6 mmol/l glucose, 2% BSA fraction V, 50 μmol/l 2-mercaptoethanol (Sigma-Aldrich, Poole, UK), 10 mmol/l nicotinamide (Calbiochem, Darmstadt, Germany), 5.5 μg/ml transferrin, 6.7 ng/ml selenite (Sigma-Aldrich), 100 units/ml penicillin and 100 μg/ml streptomicin (Lonza, Leusden, the Netherlands). The same medium, but with 2% FBS, was used after transfection with siRNAs. INS-1E cells were cultured in RPMI 1640, containing 11 mM glucose, 10% fetal bovine serum, 10 mM HEPES, 50 μM 2-mercaptoethanol, and 1 mM sodium pyruvate at 37°C with 5% CO2 in a humidified atmosphere. MIN6B1 cells were cultured in 25 mmol/l glucose DMEM supplemented by 15% fetal bovine serum, 2 mmol/l L-glutamine, 20 mM HEPES, 50 μmol/l β-mercaptoethanol, plus penicillin (100 units/mL) and streptomycin (0.1 mg/mL) at 37°C in an atmosphere of humidified air (95%) and CO2 (5%).

METHOD DETAILS

Human pancreatic islet lipoglucotoxic stress conditions and washout
After the isolation, ND islets were cultured in M199 medium (Bugliani et al., 2013; Marchetti et al., 2007), containing 5.5 mmol/l glucose, for 2 days (D2), to allow recovery from the isolation process. Then, based on previously reported procedures, (Bugliani et al., 2013; Marselli et al., 2014; Cnop et al., 2014), batches of islets were cultured for 2 additional days under one of the following metabolically stressful conditions (with islet batches from the same donor also cultured in normal M199 medium in parallel): 0.5 palmitate (P), 11.1 mmol/l glucose (g), 22.2 mmol/l glucose (G), 0.5 mmol/l palmitate + 11.1 mmol/l glucose (P+g), 0.5 mmol/l palmitate + 22.2 mmol/l glucose (P+G), 1.0 mmol/l palmitate + oleate, (1:2 molar ratio, P+O), 1.0 mmol/l palmitate + oleate + 11.1 mmol/l glucose (P+O+g), and 1.0 mmol/l palmitate + oleate + 22.2 mmol/l glucose (P+O+G). In particular, palmitate (sodium salt, Sigma Aldrich, St. Louis, MO, USA) was dissolved in 90% ethanol, heated to 60°C and 1:100 diluted to a final concentration of 0.5 mmol/l and a molar ratio of palmitate:bovine serum albumin of 3.33. A previous study showed that this corresponds to an unbound palmitate concentration of 27 nmol/l (Cnop et al., 2001). After this second 2-day incubation period (D4), batches of islets from control and metabolic stress conditions were washed and incubated with M199 medium for 4 more days (indicated respectively as D8 control and D8 washout). Altogether, 26 separate islet preparations were used, to generate results from 277 replicates.

Insulin secretion studies
Insulin secretion in response to acute glucose stimulation (3.3 and 16.7 mmol/l glucose) was assessed with 15 handpicked islets of similar size (approximate diameter 150 μm) by batch incubation (2 ml), and islet insulin content was measured after acid-alcohol extraction, as previously reported (Marchetti et al., 2007; Del Guerra et al., 2005). Insulin was quantified (μU/ml) by a radioimmunometric assay (DIAsource ImmunoAssays S.A., Nivelles, Belgium). Insulin stimulation index was calculated as the ratio of insulin release at 16.7 mmol/l glucose over release at 3.3 mmol/l glucose.

Immunocytochemistry and electron microscopy
Isolated islets were studied by light microscopy immunocytochemistry (Marselli et al., 2014) and/or electron microscopy (Masini et al., 2009; Dotta et al., 2007). For immunocytochemistry, the following primary antibodies were used: guinea pig anti-insulin antibody, 1:100, Invitrogen, Carlsbad, CA, USA; polyclonal rabbit anti-human glucagon antibody, 1:3,000, Dako, Carpinteria, CA, USA;

mouse monoclonal anti-chromogranin A antibody, 1 μg/ml, Ventana, Oro Valley, AZ, USA. Biotinylated secondary antibody, which reacts with mouse, rabbit, guinea pig and rat primary antibodies, was purchased as Histostain-Plus kits (Invitrogen). Sections were analyzed using Leica DM5500 B microscope (Leica, Wetzlar, Germany) equipped with the DFC310 FX camera (Leica). Images were acquired using Leica HCX PL FLUOTAR objective lenses at 40X magnification and Leica MetaMorph® software, v1.8.0. For electron microscopy, 30 hand-picked islet pellets were fixed with 2.5% (vol./vol.) glutaraldehyde in 0.1 mmol/l cacodylate buffer, pH 7.4 for 1h at 4°C, and then processed as detailed previously (Masini et al., 2009; Dotta et al., 2007). Apoptotic β-cells were identified based on the presence of marked chromatin condensation in the nucleus and/or blebs, as described by us and others (Masini et al., 2009; Galluzzi et al., 2007).

RNA extraction and libray preparation from the islets
Procedures were performed as previously described (Marchetti et al., 2007; Solimena et al., 2018). RNA from approximately 120 hand-picked islets per condition was prepared using the RNeasy MINI Kit + QIAshredder (QIAGEN, Hilden, Germany) through lysing and homogenizing steps followed by DNA digestion using RNase-Free DNase Set (QIAGEN) and washing steps. Total RNA concentration was measured using the NanoDrop 2000c Spectrophotometer (Thermo Fisher Scientific, Waltham, MA, USA) and RNA RIN values were obtained using Agilent Bioanalyzer 2100 (Agilent Technologies, Wokingham, UK) and Agilent RNA Nano Chips (Agilent Technologies). RIN values in the ND samples were: mean 8.9; SEM 0.1; median 8.8, range 7.9–9.7. The samples used for the T2D versus ND islet comparison had a RIN value of 7.5 and above, ensuring suitability for sequencing. Libraries were prepared using the TruSeq Stranded mRNA Library Prep Kit (Illumina, San Diego, CA, USA). Briefly, mRNA was purified from 0.40 μg total RNA using poly-T oligo attached magnetic beads, and was then fragmented and primed with random hexamers for reverse transcription. Second strand synthesis was performed by incorporating dUTP in place of dTTP to generate blunt-ended ds cDNA. Adenylation of the 3′ ends and adaptor ligation were then performed. Selective enrichment of DNA fragments with adaptor molecules on both ends and DNA amplification were obtained by PCR. The generated libraries were quantified using qPCR and quality was assessed using Agilent Bioanalyzer 2100 (Agilent Technologies) and Agilent DNA 1000 chips (Agilent Technologies). All the libraries had concentration and size (300 bp) suitable for sequencing, which was performed on the Illumina HiSeq 2500 instrument (Illumina) for the lipoglucotoxic conditions, and on an Illumina Genome Analyzer II (GAII, Illumina) for the T2D and ND samples. Paired-end sequencing (2x100bp) at 170 million reads was performed.

Validation studies: Proteomics experiments
Proteomics experiments (Ciregia et al., 2017) were accomplished with human islets to verify the protein expression of some of the differentially expressed genes, and functional as well as molecular experiments were conducted to validate the role of genes associated with changes in insulin secretion in the human islet incubation conditions described above. For shotgun proteomics analysis, experiments were performed similar to what previously described (Giusti et al., 2019; Ciregia et al., 2017; Ronci et al., 2018; Pieragostino et al., 2019). Aliquots of 40 μg of human islets protein extracts were loaded onto 12% acrylamide resolving gel and subjected to 1D-electrophoresis. After protein visualization by Coomassie blue, gel bands (16 bands for lane) were excised, destained and subjected to in-gel reduction, alkylation and overnight trypsin digestion at 37°C. The resulting peptides were analyzed in technical triplicates by LC-MS/MS using a Proxeon EASY-nLCII (Thermo Fisher Scientific, Milan, Italy) chromatographic system coupled to a Maxis HD UHR-TOF (Bruker Daltonics GmbH, Bremen, Germany) mass spectrometer equipped with a nanoESI spray source. Peptides were loaded on the EASY-Column C18 trapping column (2 cm L., 100 μm I.D, 5 μm ps, Thermo Fisher Scientific), and subsequently separated on an Acclaim PepMap100 C18 (75 μm I.D., 25 cm L, 5 μm ps, Thermo Fisher Scientific) nano scale chromatographic column. The flow rate was set to 300 nL/min and the gradient was from 3 to 35% of B in 80 min followed by 35 to 45% in 10 min and from 45 to 90% in 11 min. Mobile phase A was 0.1% formic acid in H_2O and mobile phase B was 0.1% formic acid in acetonitrile. The mass spectrometer was operated in positive ion polarity and Auto MS/MS mode (Data Dependent Acquisition - DDA), using N2 as collision gas for CID fragmentation. Precursors in the range 350 to 2,200 m/z (excluding 1,220.0–1,224.5 m/z) with a preferred charge state +2 to +5 (excluding singly charged ions) and absolute intensity above 4,706 counts were selected for fragmentation in a maximum cycle time of 3 s. After acquiring one MS/MS spectrum, the precursors were actively excluded from selection for 30 s. Isolation width and collision energy for MS/MS fragmentation were set according to the mass and charge state of the precursor ions (from 3 to 9 Da and from 21 eV to 55 eV). In-source reference lock mass (1,221.9906 m/z) was acquired online throughout the runs.

Validation studies: ANKRD23 experiments
To assess the effect of Ankrd23 overexpression on AMPK activation (Martinez-Sanchez et al., 2018)), the MIN6B1 cells were plated on a 12-well plate, in duplicate for each condition and infected by an adenovirus expressing either GFP (control) or mouse Ankrd23 (Vector Biolabs, Malvern, PA, USA) at a multiplicity of infection (MOI) of 10 virus particle/cell. Two days post-infection, the cells were preincubated for 1h in Krebs Ringer Bicarbonate HEPES (KRBH) buffer (40 mM NaCl, 3.6 mM KCl, 0.5 mM NaH_2PO_4, 0.2 mM $MgSO_4$, 1.5 mM $CaCl_2$, 10 mM HEPES, 25 mM $NaHCO_3$), saturated with 95% O_2/5% CO_2 and adjusted to pH 7.4 with the addition of 3 mM glucose before incubation for 30 min in low (3 mM) or high (30 mM) glucose. The cells were then lysed in 100 μL Radioimmunoprecipitation assay buffer (RIPA) containing protease (cOmplete Protease Inhibitor Cocktail, Roche) and phosphatase inhibitors (phosphatase inhibitor cocktail 2, Sigma). Protein concentration was assessed using a Pierce BCA protein assay kit (Thermo Fisher Scientific) according to manufacturer's instructions. Proteins were separated by SDS-PAGE under reducing conditions and transferred onto a polyvinylidene fluoride membrane (0.45 μm, Amersham). The membrane was blocked in 5% milk in PBS-T0.1

(Phosphate Buffer Saline, Tween 0.1%) for 1h and incubated overnight at 4°C with the primary antibodies anti-pAMPK (Abcam 2535S, dilution 1/1000), pRaptor (Abcam 2083S, dilution 1/1000), pACC (Abcam 3661S, dilution 1/1000), AMPK (Abcam 2532S, dilution 1/1000), Raptor (Abcam 2280S, dilution 1/1000), ACC (Abcam 3662S, dilution 1/1000), ANKRD23 (Abcam ab118210, dilution 1/500). The expression of α-tubulin (dilution 1/20000; T5168, Sigma) was used as a loading control. After washing, the membrane was incubated for 1h in horseradish peroxidase coupled secondary antibodies (Goat Anti-Rabbit-HRP, Abcam, AB6721, dilution 1/8000) and the signal was detected on Amersham Hyperfilm ECL, after exposure to Amersham ECL WB Detection Reagent. Band intensity was measured using ImageJ.

Validation studies: Sec61G experiments

The role of Sec61G was evaluated in INS-1E and EndoC-βH1 cells, cultured as described (Asfari et al., 1992; Ravassard et al., 2011; Brozzi et al., 2015) and further validated in dispersed human islets. Cells were transfected overnight with 30 nM control siRNA (QIAGEN) or siRNAs targeting rat or human Sec61G as previously described (Moore et al., 2012). Messenger RNA was isolated using the Dynabeads mRNA DIRECT kit (Invitrogen, Paisley, UK) and reverse transcribed (Cardozo et al., 2005). qRT-PCR was done using iQ SYBR Green Supermix (BIO-RAD, Nazareth Eke, Belgium) on a LightCycler (Roche Diagnostics, Mannheim, Germany) or iCycler MyiQ Single Color (BIORAD). Data were expressed as number of copies generated from the standard curve method and corrected for the reference gene β-actin or glyceraldehyde-3phosphate dehydrogenase (GAPDH). Primers used for qRT-PCR are listed in the table below. Cells were exposed to 0.5 mM palmitate pre-complexed to 0.67% FFA-free BSA (16h for INS-1E cells, 24h for human islet cells) or to thapsigargin for 24h. Apoptosis was assessed by fluorescence microscopy in propidium iodide (5 mg/ml) and Hoechst 33342 (5 mg/ml) stained cells as described (Cnop et al., 2007). For western blotting, INS-1E cells were lysed in Laemmli buffer and immunoblotted with cleaved caspase 3 (Asp175, Cell Signaling Cat# 9661, dilution 1/1000), cleaved caspase 9 (Asp353, Cell Signaling Cat# 9507, 1/1000), and tubulin (Sigma Cat# T9026, 1/5000) antibodies. Membranes were subsequently exposed to secondary peroxidase-conjugated antibody (1/5000), and developed using SuperSignal West Femto chemiluminescent substrate (Thermo Scientific) in a Bio-Rad chemi DocTM XRS + (Bio-Rad laboratories).

Primers for rat and human GAPDH, ACTB, SEC61G

	Application	Forward (5'-3')	Reverse (5'-3')	Species	Length
GAPDH ST	Standard curve	ATGACTCTACCCACGGCAAG	TGTGAGGGAGATGCTCAGTG	Rat	930 bp
ACTB ST	Standard curve	AAATCTGGCACCACACCTTC	CCGATCCACACGGAGTACTT	Human	805 bp
SEC61G ST	Standard curve	TGGATCAGGTAATGCAGTTTG	TAGGGATGTGGATCAGTTTCA	Rat	180bp
SEC61G ST	Standard curve	TGGATCAGGTAATGCAGTTTG	CAGCCACCAACAATGATGTT	Human	205 bp
GAPDH RT	Real time	AGTTCAACGGCACAGTCAAG	TACTCAGCACCAGCATCACC	Rat	136 bp
ACTB RT	Real time	CTGTACGCCAACACAGTGCT	GCTCAGGAGGAGCAATGATC	Human	127 bp
SEC61G RT	Real time	AGT CGG CAG TTT GTA AAG GA	GAA CCC CAT GAT AGC GAA T	Rat	117 bp
SEC61G RT	Real time	CGG CAG TTT GTA AAG GAC TC	GCC AAT GAA TCC CAT TAT AGC	Human	120 bp

QUANTIFICATION AND STATISTICAL ANALYSIS

RNA-seq data analysis

Sequenced reads from lipo/glucotoxicity experiments were mapped to the human genome (assembly version GRCh37/hg19) using TopHat 2 (v2.0.13) (Kim et al., 2013) with default parameters. Reads were assigned to their corresponding exons and genes based on GENCODE annotation v18 (Frankish et al., 2019) using Flux Capacitor (Montgomery et al., 2010) with default parameters. Resulting raw gene counts were normalized to gene length (sum of exons) and sequencing depth, i.e., reads per kilobase per million (RPKM) mapped reads. The differentially expressed genes were identified by the R/Bioconductor package EdgeR (Robinson et al., 2010) using the raw counts with a false discovery rate (FDR) < 0.05 as cut-off for significance. The p value for EdgeR differential analysis were corrected according to the Benjamini and Hochberg 1995 method, as implemented by R p.adjust function (Benjamini and Hochberg, 1995). For the comparison of differential expression of lipo/glucotoxicity versus T2D, sequence reads were quantified with Salmon 13.2 (Patro et al., 2017) using the transcriptome GRCh38 version 95 in quasi-mapping mode with sequence and GC bias corrections and mapping validation. Differential analysis was done using R DESeq2 package version 1.24.0 (Love et al., 2014). The enrichment map and gene list and plots were generated by a modified two-tailed Rank-Rank Hypergeometric Overlap (RRHO) method (Plaisier et al., 2010; Cahill et al., 2018). The logarithm of fold change was used to rank differentially expressed genes. For the within-group comparisons over time, we first evaluated time-induced effects by performing differential transcription analysis for the control conditions between D4 versus D8, which reflects time-induced effects in the absence of a metabolic insult. We next examined the number of differentially expressed genes common to treatment and control, and the magnitude of change over time. We considered differentially expressed those genes with larger fold change of expression by treatment than control/time as "true" differentially expressed genes. We also took into account the time effect in the RRHO analyses. To do so, we computed a corrected fold change

(FCcorr). From the fold change of D4 P ± G (FCa) versus D4 control and D8 P ± G versus D8 control (FCb), FCcorr is given by FCb/FCa. The RRHO software was modified to better take into account the multiplicity of minimal p values, null p values and the asymmetry between the number of genes up- or downregulated in the two datasets. The p value for RRHO where controlled for multiple testing with the Benjamini and Yekutieli method (2001) as implemented by R p.adjust function (Benjamini and Yekutieli, 2001). The functional enrichment analysis for the RRHO gene lists was generated with the gprofiler2 R package (Raudvere et al., 2019).

Evaluation of functional enrichment

Functional enrichment was generated using Gene Set Enrichment Analysis (GSEA) software v3.0 (Subramanian et al., 2005). Standard parameters were applied, except for minimum and maximum size of functional category values that were adjusted to 5 and 500, respectively. Enrichment maps of significantly modified biological processes (Gene Ontology) were generated using the plugin "Enrichment Map" v3.1 (Merico et al., 2010; Isserlin et al., 2010) and visualized within Cytoscape v3.6, using as geneset similarity cutoff a Jacard Index of 0.25 and a FDR < 0.05. To identify genes most likely to be relevant to the clusters of genesets produced by Enrichment Mapping, we identified the genes most frequently appearing across their leading-edge analysis (Subramanian et al., 2005). The leading-edge subset represents the core of genes accounting for the gene set's enrichment signal in GSEA. Heatmaps showing GSEA rank metric scores from these genes are represented, higher absolute values identify critical genes.

Proteomic data analysis

For bioinformatics processing, raw data were processed using PEAKS Studio v7.5 software (Bioinformatic Solutions Inc, Waterloo, Canada) using the 'correct precursor only' option. The resulting mass lists were searched against nextprot database (including isoforms as of June 2017; 42,151 entries). Carbamidomethylation of cysteines was selected as fixed modification, oxidation of methionines and deamidation of asparagine and glutamine were set as variable modifications. Non-specific cleavage was allowed to one end of the peptides, with a maximum of 2 missed cleavages. The highest error mass tolerances for precursors and fragments were set at 10 ppm and 0.05 Da, respectively.

Expression quantitative trait loci (eQTL) analysis

Details of the study were published recently (Khamis et al., 2019). Briefly, an eQTL analysis was performed in a total of 100 islets from ND organ donor subjects. Genotyping was performed using the 2.5 M Omniarray Beadchip and RNA analysis was performed using Human Genome U133 Plus 2.0 Array to generate the eQTL analysis. Gender and age were used as covariates and a cis-window of 500 kb was used. A nominal p value of $p < 0.05$ was considered significant.

Statistical analysis

The other results are presented as mean ± SE, unless otherwise indicated, and were analyzed with the R software or the GraphPad Prism Software v8.4.2. Comparisons between two sets of data were performed by the two-tailed Student's t test. Results from more than two groups were analyzed by ANOVA followed by the Tukey correction. Multiple linear regression was used to take into account the effects of incubation time and culture conditions on multiple groups of islets. A p value < 0.05 was considered statistically significant.